

Review

## Machine learning algorithms for defect detection in metal laser-based additive manufacturing: A review



Yanzhou Fu<sup>a,\*</sup>, Austin R.J. Downey<sup>a,b</sup>, Lang Yuan<sup>a</sup>, Tianyu Zhang<sup>a</sup>, Avery Pratt<sup>c</sup>, Yunusa Balogun<sup>c</sup>

<sup>a</sup> Department of Mechanical Engineering, University of South Carolina, Columbia, SC 29208, United States

<sup>b</sup> Department of Civil and Environmental Engineering, University of South Carolina, Columbia, SC 29208, United States

<sup>c</sup> Naval Surface Warfare Center, Crane Division, Crane, IN 47522, United States

### ARTICLE INFO

**Keywords:**

Laser-based additive manufacturing  
Machine learning  
Defect detection  
Product quality  
Artificial intelligence

### ABSTRACT

Laser-based additive manufacturing (LBAM), a series of additive manufacturing technologies, has unrivaled advantages due to its design freedom to manufacture complex parts with a wide range of applications. Although advancements in LBAM processes and materials have led to increased manufacturing capabilities, the printing process's repeatability, durability, and reliability still face significant challenges. Therefore, a defect detection system for the LBAM processes is essential, as it promises to guarantee product quality and increase the efficiency of the printing process. As a practical and widely applied technology, machine learning methods have been providing novel insights into the manufacturing process, which has proven advantages for defect detection in LBAM. This paper summarizes the machine learning algorithms for defect detection in the metal LBAM processes. To have a comprehensive and systematic summary, machine learning algorithm, material type, defect type, dataset type, and algorithm accuracy for various LBAM technologies are described.

### 1. Introduction

Additive manufacturing (AM) is a rapidly growing technology that has proven advantages for unlocking design freedom for lightweight components with complex geometries and as a disruptive technology, it offers exciting new manufacturing capabilities [1,2]. AM has been actively utilized in various industries, and it shows enormous economic potential [3,4]. According to the Wohlers 2021 Report on AM, in 2020, the AM industry grew 7.5%, or nearly \$ 12.8 billion, despite the global COVID-19 pandemic [5]. Among various AM techniques, laser-based additive manufacturing (LBAM) displays considerable potential for industrial adoption and has already changed the manufacturing process by enabling complex design and innovative application development [6]. The principle of LBAM technologies lie in using a laser beam to yield thermal energy for sintering/melting and consolidating additive materials or emitting light quanta of a particular wavelength to induce a chemical curing response in vat polymerization. The materials utilized in the LBAM processes can be in the form of powders (metals, ceramics, and polymers), solids (paper, plastics, and metals), or liquids (resin). In LBAM, according to the difference in material feeding approach, there

are three major systems: powder blown system, powder bed system, and wire-feed system. In the powder blown system, the material is carried out through single or multiple nozzles and melted by a laser beam. The powder bed system generally has two chambers, a build chamber for printing and a powder chamber with a coating roller to spread the powder material across the build chamber. In the wire-feed system, the wire is fed and melted to manufacture the metal parts.

Due to the convenience of fabrication and the practicability of mechanical properties enhancement, LBAM is regarded as a highly favored manufacturing technology for Industry 4.0 over conventional technologies [7]. However, its full potential is held back by variabilities inherent to the process. The LBAM processes are dominated by complicated physics processes, including laser energy absorption and transmission, material evaporation, remelting and solidification, melt pool fluid dynamics, and microstructure evolution via epitaxial growth and nucleation. Defects, such as cracks, pores, distortion, and insufficient melt frequently occur in the printing process, impacting the manufactured parts' mechanical and functional properties. The severity and density of these defects can be seen as a semi-stochastic function of material parameters and printing parameters related to laser energy density and its associated parameters, such as power, speed, and spot

\* Corresponding author.

E-mail address: [yanzhouf@email.sc.edu](mailto:yanzhouf@email.sc.edu) (Y. Fu).

<b>Nomenclature</b>	
AI	artificial intelligence
AM	additive manufacturing
ANN	artificial neural network
BC	Bayesian classifier
CNN	convolutional neural network
DBN	deep belief network
DCNN	deep convolutional neural network
DED	directed energy deposition
DL	deep learning
DMLS	direct metal laser sintering
DNN	deep neural network
DT	decision Tree
GMM	Gaussian mixture model
GP	genetic programming
KMC	K-means clustering
KNN	K-nearest neighbor
LBAM	laser-based additive manufacturing
LDA	linear discriminant analysis
LENS	laser engineered net shaping
LMD	laser metal deposition
LPBF	laser powder bed fusion
LR	linear regression
LS-SVM	least square support vector machine
LSTM	long short-term memory
ML	machine learning
PBF	powder bed fusion
PCA	principal component analysis
QDA	quadratic discriminant analysis
RF	random forests
RL	reinforcement learning
RMSE	root-mean-square error
RNN	recurrent neural network
SLM	selective laser melting
SOMs	self-organized maps
SVM	support vector machine

size [8]. In addition to the above factors, the LBAM process consists of different print technologies. Even though they share the same basic principle, individual characteristic are exhibited by different LBAM processes, which makes defect detection harder. Also, part geometry and the specific powder utilized for fabrication influence defect formation dramatically, making defect detection in LBAM complicated and challenging. To accelerate the industrialization of the LBAM processes, a novel and effective defect detection system to detect and eliminate defects and guarantee product quality is essential.

Machine learning (ML) has progressed from a laboratory curiosity to a fundamental process used in various industries and fields, including smart manufacturing [9,10], civil engineering [11], and biomedical science [12]. For the LBAM processes, ML has proven itself as a useful way to monitor product quality or detect defects [13]. Applying ML to a defect detection system offers new insights into LBAM processes due to its ability to discover implicit knowledge and build the relationship between printing parameters and product quality [14].

This paper reviews and summarizes the latest ML algorithms that have been utilized for LBAM defect detection systems, examines the achievement of these systems, and discusses the current and future research direction. It is important to point out that this paper only focuses on metal LBAM processes. In the author's search, no defect detection ML algorithms for laser-based wire-feed systems were found; all research focused on powder blown systems and powder bed fusion systems. Powder blown system is commonly known as directed energy deposition (DED), laser metal deposition (LMD), or laser engineered net shaping (LENS), while powder bed fusion system, is commonly known as laser powder bed fusion (LPBF), direct metal laser melting (DMLM), direct metal laser sintering (DMLS), or selective laser melting (SLM). As these technologies essentially are the same, DED will be used for all powder blown systems and LPBF for all powder bed fusion processes to unify the naming conventions. To have a systematic and comprehensive summary, ML algorithm, material type, defect type, input data type, and algorithm accuracy for various LBAM technologies are described. In this paper, the background is described in Section 1, and Section 2 presents different defect types in the LBAM processes. In Section 3, ML algorithms used in defect detection systems for the LBAM processes are discussed; a future trend and conclusion to the review are discussed in Section 4 and Section 5.

## 2. Defect types in LBAM

Although different LBAM processes have their own characteristics,

they share similar manufacturing methodologies. The two most common technologies for LBAM are DED and LPBF and are shown in Fig. 1. As shown in Fig. 1(a), the center of a typical DED system is the nozzle head, which consists of the energy source (e.g., laser beam, electron beam) to melt additive material at the point of deposition and the material delivery nozzle for feeding powder or wire [15]. Typically, the nozzle head is fixed on either an articulated arm or a multi-axis computer numerical control (CNC) head. The laser beam melts the powder/wire and forms the melt pool on the substrate at the start spot along the build track. This process continues until the whole part is completed. The LPBF system is shown in Fig. 1(b). In the LPBF printing process, the laser beam scans at a controlled speed on the powder bed, and the selected locations of the powder are fused to form a solid track. The powder bed is sunk by the predefined layer thickness, and a new powder layer is spread and leveled after the previous layer is finished. The process repeats until the part is completely built. As the LBAM processes are complicated; many printing parameters, such as laser scan speed, laser power, scanning pattern, material type and size, and chamber environment, are involved in this process. Any improper settings in printing will produce defects. These defects can be divided into four types: product geometric and dimensional defect, porosity, incomplete fusion, and cracks. This section describes defect types and is organized as follows: Section 2.1 shows the geometric and dimensional defect, Section 2.2 presents the porosity defect, incomplete fusion is described in Section 2.3, and Section 2.4 discusses the crack defect.

### 2.1. Geometric and dimensional defects

Geometric deviation is one of the common defects in the LBAM processes. Geometric defects may be caused by machine errors and errors in the generation of machine code that controls laser movement. Laser position error and platform movement error are two machine errors that lead to geometric defects [16]. Layer-based slicing can introduce step-wise marks on surfaces, where their contours may also introduce inaccuracy due to melt pool dimensions.

For dimensional inaccuracy, the main influence factor is shrinkage/distortion. In the LBAM processes, there are two kinds of shrinkage: sintering shrinkage and thermal shrinkage. Sintering shrinkage is mainly produced by densification, while thermal shrinkage is caused by cyclic heating and cooling, which leads to significant residual stress, thus, local plastic deformation [17,18,19]. An example of a distorted canonical geometry is shown in Fig. 2, where shrinkage was observed near the top.

Another factor influencing product geometric and dimensional

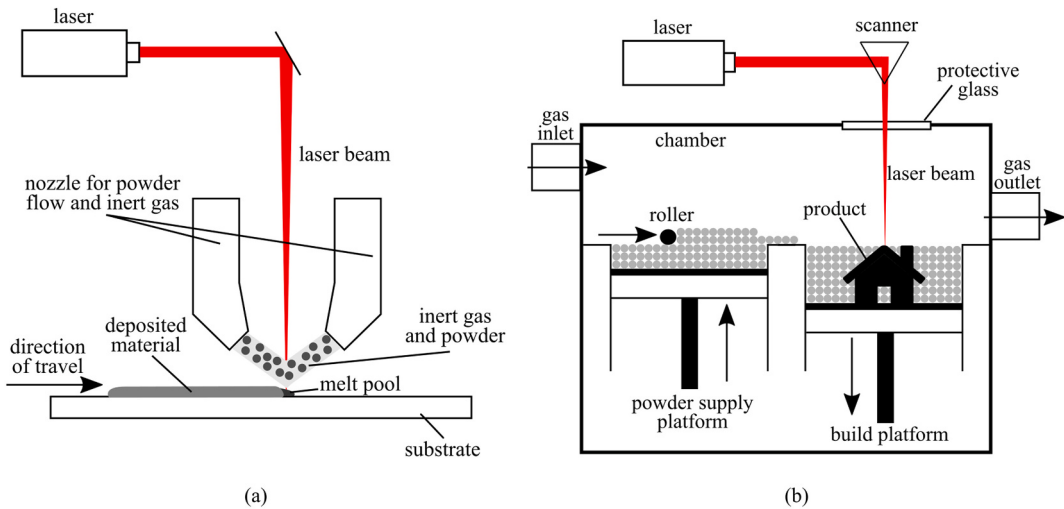


**Fig. 1.** Schematic illustration of LBAM processes with two different feeding systems: (a) the DED technology of the powder blown system; and (b) the LPBF technology of the powder bed fusion system.

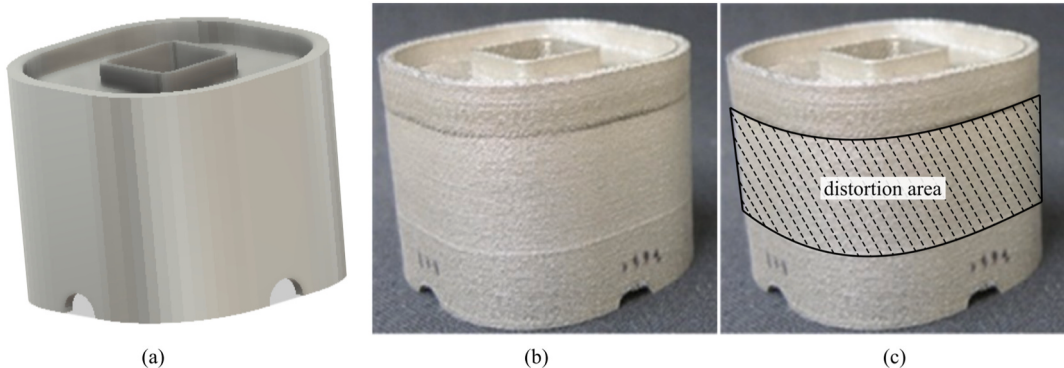


**Fig. 2.** An distorted product of LPBF process with stainless steel 316L: (a) CAD model of the designed product; (b) manufactured product; and (c) the distortion area on the manufactured product.

accuracy is surface finish accuracy, also known as surface roughness [20]. During the printing process, partially melted particles and spatters attach to the product surface, causing the final dimension to vary from that designed [21]. Poor surface roughness not only impacts the product's usefulness but also influences the material's properties (e.g., fatigue life) [22]. Fig. 3 shows a typical surface morphology of the LPBF process in 316L stainless steel, where melt pool tracks and attached particles can be observed.

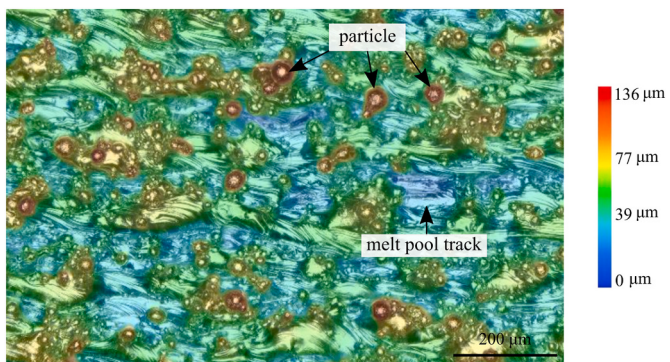


**Fig. 3.** Product's surface metrology of LPBF process with stainless steel 316L.

## 2.2. Porosity

Porosity is a common defect in the LBAM processes and negatively impacts product density [23]. It is particularly deleterious to mechanical properties, such as fatigue for structural components. The porosity size varies with distinguishing shapes under different forming mechanisms [24]. Typically, pores form due to insufficient powder spreading, lack of fusion (as part of the “incomplete fusion defect” discussed next), keyholing, shrinkage, and gas involvement. The first three types are large in size and are due to improper process parameters. For example, low metal powder packing density (e.g., less than 50%) and spatters may lead to large voids in the powder bed, which cannot be filled during melting. High laser energy density leads to keyholing, and metal vapor pressure results in pores at the bottom of the deep melt pool. Through optimization of LBAM processes parameters, these defects can be fully eliminated [25]. The latter two types, in general, are smaller in size. Pores due to solidification shrinkage are normally located between grains and follow the shape of grain boundaries [26]. Gas-induced pores are spherical in shape and can possibly originate from the gas trapped in the powder feedstock particles due to the gas-atomized process, gas dissolved in metal due to different gas solubility at different temperatures, metal vapor generated during melting, or moisture from the powder surface. An example of porosity is shown in Fig. 4. This type of pores cannot be completely avoided due to the nature of its forming mechanism.

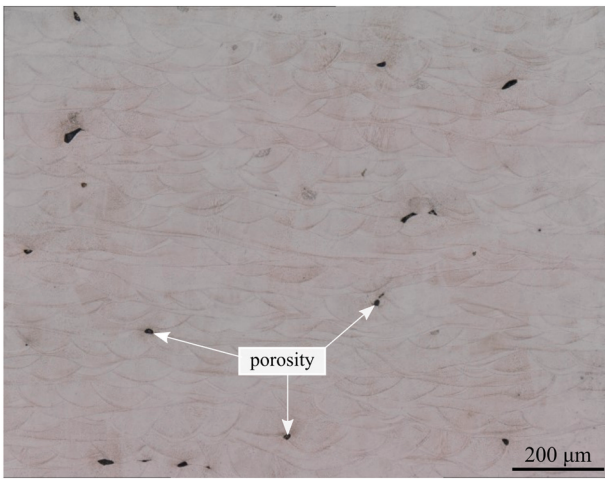


**Fig. 4.** Optical image of porosities in LBAM printing part with stainless steel 316L.

### 2.3. Incomplete fusion

The incomplete fusion hole is mainly produced by a lack of energy input in the LBAM printing processes, also known as lack of fusion defects, as shown in Fig. 5. Lack of fusion defects are produced mainly because the metal powder is not fully melted to deposit a new layer on the previous layer with sufficient overlap between them [27,28]. The lack of fusion defects can be categorized into two types: poor bonding defects formed by insufficient molten metal powder in a solidification process and defects due to unmelted metal powder. It is also one of the reasons for large pores in LBAM.

When the scan path of the laser density is low, the molten pool width is small, which produces an insufficient overlap between each track. The insufficient overlap then results in unmelted metal powder between the scan tracks as there is insufficient energy to fully melt the powder for a new layer [29]. As a result, incomplete fusions are produced and unmelted powder remains in the LBAM printed product, especially between the scan tracks and the deposited layers. Moreover, the defect formation area makes the product surface rough, directly impacting the molten metal's flow to form interlayer defects. Then the interlayer defects may gradually extend and propagate to form more significant multi-layer defects in the continuing printing process [30].

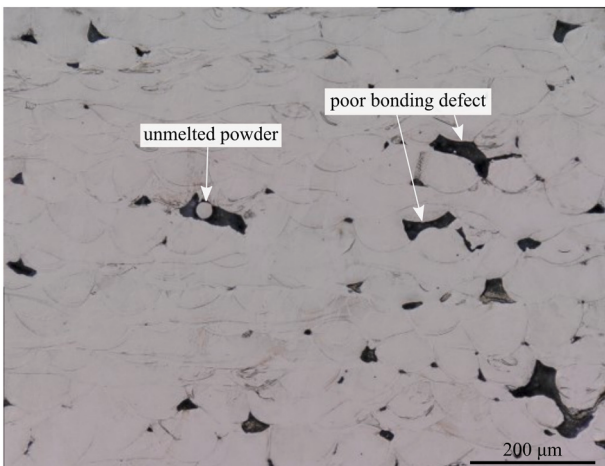


**Fig. 5.** Optical image of the lack of fusion defects in LBAM printing part with stainless steel 316L.

### 2.4. Cracks

In the LBAM printing processes, with a high laser energy input, the metal powder undergoes fast-melting and rapid solidification. The cooling rate in the melting pool can reach more than  $1.6 \times 10^6$  K/s following high-temperature gradients [31]. Cracks initiate during and after solidification based on the materials, processes, and part design. For example, solidification cracking forms due to insufficient liquid feed at the last stage of solidification. Strain-age cracking, a type of ductile cracking, forms due to the formation of precipitates during heat treatment processes. Also common is the tremendous amount of residual stress developed in the printed product, which may exceed the ultimate strength of the materials and lead to cracks [32,33]. In Fig. 6(a), solidification cracking was developed along grain boundaries in the LPBF printing process fabricated part. Fig. 6(b) shows the enlarged crack morphology of the red box in Fig. 6(a).

## 3. Machine learning algorithms for defect detection

ML is a subset of artificial intelligence (AI) that provides systems the capacity to learn and improve from experience without being explicitly programmed. Lots of the ML models have been built and applied by researchers for defect detection in AM [14]. This section reports ML algorithms used explicitly for defect detection during the metal LBAM processes. The field of ML can generally be divided into four domains, as shown in Fig. 7: 1) supervised machine learning; 2) unsupervised machine learning; 3) semi-supervised machine learning, and; 4) reinforcement machine learning. This section presents the state-of-the-art in defect detection and is organized by domain: Section 3.1 presents supervised machine learning algorithms; Section 3.2 describes unsupervised algorithms; Section 3.3 lists the semi-supervised machine learning algorithms; and Section 3.4 discusses reinforcement learning algorithms.

### 3.1. Supervised learning

Supervised learning is the most widely used ML technique. The training dataset needs to be labeled with input values and the corresponding output values. During the training process, the ML algorithm uses this labeled dataset and learns the relationship between input data and output data. Supervised learning is appropriate for classification and regression; therefore, many defect detection systems use supervised learning approaches to detect and classify different defects in LBAM. For clarity, the supervised learning subsection of this paper is divided into three parts: traditional classifier, artificial neural network (without convolutional layers), and convolutional neural network. As most of the reviewed research utilizes several classification algorithms in one paper and compare their performance, this paper lists all traditional classification algorithms together. Traditional classification algorithms include support vector machine, Bayesian classifier, logistic classification, K-nearest neighbors, and decision tree. Artificial neural network (ANN) can also be formulated as a classifier and are discussed here in detail with one subsection. Furthermore, ANNs that utilize convolutional layers in their architectures are separated into their own subsection due to their prevalence in the literature. Table 1 compiles a list of supervised ML algorithms utilized for detecting defects in components manufactured using the LBAM processes. In Table 1, key features of the reviewed research are listed, including ML domain, dataset type, material type, defect type, and algorithm performance.

#### 3.1.1. Traditional regression

Regression is a method of modeling target values based on independent predictors. This method is mainly used to uncover cause and effect relationships between variables. Regression techniques differ primarily depending on the number of independent variables and the relationship between the dependent and independent variables.

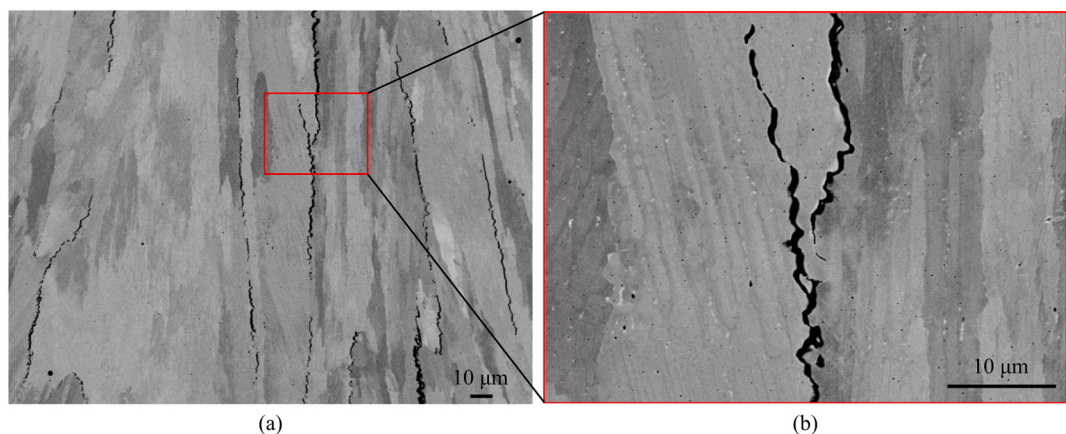


**Fig. 6.** Image of crack morphology from an LBAM fabricated part with stainless steel 316L: (a) crack morphology; and (b) enlarged crack morphology.

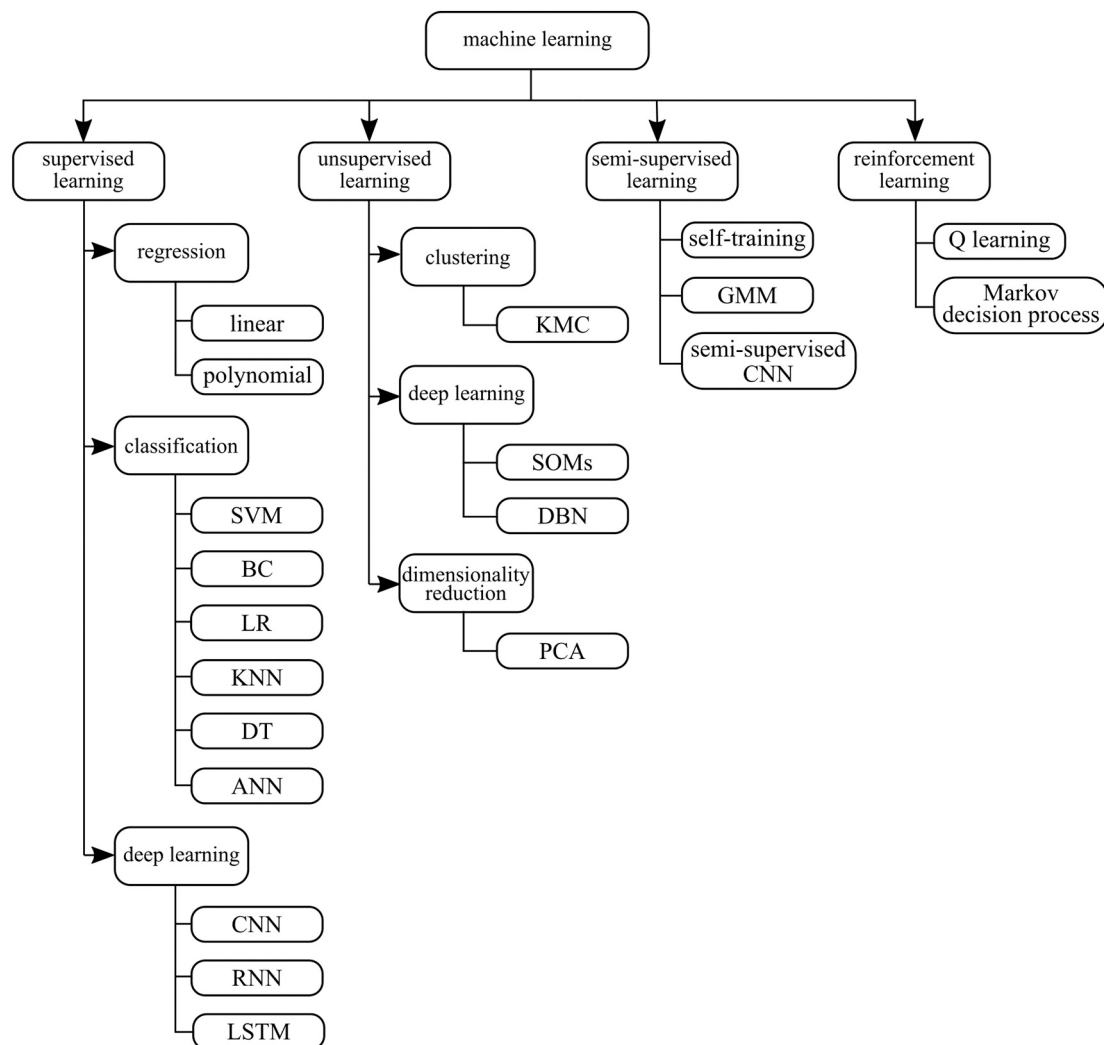


**Fig. 7.** Categories of different machine learning algorithms (all the abbreviations are listed in the nomenclature and can be found in the paper).

Regression algorithms may be linear as well as non-linear.

Different regression algorithms also have been applied to defect detection in the LBAM process. Mahmoudi et al. built an anomaly detection system for the LPBF printing process [34]. This system detects printing process deviations by using the thermal signals obtained from the thermal images of the melt pool. Logistic regression is utilized to

decide the printing process quality (in control or out of control) through a step-by-step process. The result shows this framework had a very low error rate for cavity defect detection, which can detect the 750  $\mu\text{m}$  diameter cylindrical cavity on a 5.5  $\times$  8  $\times$  9 mm rectangular prism printed by 17-4 precipitation hardening stainless steel powder. Gaja et al. used a logistic regression model to detect product defects simulated

**Table 1**

Supervised ML algorithms utilized in defect detection for LBAM processes.

ML category	ML algorithm	AM technology	Material type	Defect type	Dataset type	Accuracy	Reference
Supervised learning	Logistic regression	LPBF	17-4 precipitation stainless steel	Anomalous, good quality	Melt pool thermal image	99.6%	[34]
		DED	Mixing Ti-6Al-4V with H13 tool steel	Pore, crack	AE signal	1.72973 (MSE)	[35]
	Gaussian process regression	LPBF	17-4 stainless steel	Porosity	Laser power, scanning speed	No specific accuracy	[36]
	Support vector machine	LPBF	Stainless steel 304L	Underheating, medium underheating, normal, medium overheating, overheating	Acoustic signal	89.13%	[37]
		DED	Ti-6Al-4V	Porosity	Melt pool thermal image	97.97%	[38]
	LPBF	17-4 precipitation stainless steel	Anomalous, good quality		Melt pool thermal image	99.5%	[34]
		DED	Ti-6AL-4V.	Healthy layer, unhealthy layer	Melt pool thermal image	91.65%	[39]
	LPBF	Inconel 718	Desirable, balling, severe keyholing, keyholing porosity, or under-melting		Melt pool morphology	85.1%	[40]
		Stainless steel GP-1	Anomalous, good quality		Layerwise optical imaging	80%	[41]
	LPBF	Ti-6Al-4V	Porosity		Layerwise optical imaging	89.36%	[42]
Bayesian classifier	LPBF	Stainless steel 316L	Track continuity		Optical image	90.1%	[43]
	LPBF	Stainless steel GP-1	Anomalous, good quality		Optical image	85%	[44]
	DED	Stainless steel 316L	Track depositing height		Printing parameters	2.89E-08 (MSE)	[45]
	LPBF	Inconel 625	Porosity, quality of fusion		Visual image	89.5%	[46]
	LPBF	AlSi10Mg aluminum powder	Key hole, lack of fusion		Optical image	77%	[47]
	DED	Ti-6Al-4V	Porosity		Melt pool thermal image	98.44%	[38]
	LPBF	Ti-6Al-4V	Porosity		Layerwise optical imaging	78.60%	[42]
	LPBF	17-4 precipitation stainless steel	Anomalous, good quality		Melt pool thermal image	99.1%	[34]
	LPBF	Inconel 718	Porosity		Photodetector data	90%	[48]
	LPBF	Stainless steel 316L	No defect, bulge defect, dent defect, wavy defect		Point cloud	93.15%	[49]
Random decision tree	DED	Al-5083 powder	Macropores, micropores, elongated pores		Optical microscope image	94.41%	[50]
Artificial neural network	LPBF	Stainless steel GP-1	Anomalous, good quality		Layerwise optical imaging	90%	[41]
Convolutional neural network	LPBF	Ti-6Al-4V	Porosity		Layerwise optical imaging	84.40%	[42]
	DED	Mixing Ti-6Al-4V with H13 tool steel	Pore, crack		AE signal	1.702703 (MSE)	[35]
	LPBF	Inconel 625	Surface texture		Printing process parameters	Refer to paper	[51]
	LPBF	Stainless steel 316L	Balling, lack-of-fusion, conduction, key hole		Pyrometer data, video camera data	Refer to paper	[52]
	LPBF	Ti-6Al-4V	Geometry variation		Layerwise image	92.50 ± 1.03%	[53]
	LPBF	Titanium alloy, STM B348 Grade 23 Ti-6Al-4V	Printing condition variation		Powder bed image	97.14%	[54]
	LPBF	Stainless steel 316L	Track continuity		Optical image	92.7%	[43]
	DED	Stainless steel 304, stainless steel 316, Ti-6Al-4V, AlCoCrFeNi alloys, Inconel 718	Good quality, crack, gas porosity, lack of fusion		Digital microscope image	92.1%	[55]
	LPBF	Ti-6Al-4V	Thin wall's thickness, density, edge smoothness, discontinuity		Optical image	85%	[56]
	LPBF	CL 31	Good quality, average quality, bad quality		QM-meltpool 3D-generated image	98.9%	[57]
(continued on next page)	LPBF	Stainless steel 316L	Track continuity		Printing process video	93.1%	[58]
	LPBF	ASTM F75 I CoCrMo	Under-melt, beautiful-weld, over-melt		Micrograph image	100%	[59]
	DED	Stainless steel 316L	Dilution		MWIR image	2.8% (RMSE)	[60]
	DED	Sponge titanium powder	Porosity		Melt pool image	91.2%	[61]
	DED	Stainless steel 304, stainless steel 316, Ti-6Al-4V, AlCoCrFeNi	Gas porosity, crack, lack of fusion		Optical image	92.1%	[55]
	DED	Ti-6Al-4V	Porosity		Pyrometer image	100%	[62]
	DED	0Cr18Ni9 powder	Printing parameter variation		Thermal image	80%	[63]

**Table 1** (continued)

ML category	ML algorithm	AM technology	Material type	Defect type	Dataset type	Accuracy	Reference
Long-term recurrent convolutional networks	LBPF	AlSi10Mg, bronze, Inconel 625, Inconel 718, stainless steel 316L, Ti-6Al-4V, Fe—3Si, stainless steel 17-4 PH	AlSi10Mg, bronze, Inconel 625, Inconel 718, stainless steel 316L, Ti-6Al-4V, Fe—3Si, stainless steel 17-4 PH	Recoater hopping, recoater streaking, porosity, swelling, spatter, soot, debris, super-elevation, part damage, incomplete spreading	Powder bed image	Refer to paper	[64]
	LPBF	Alloys, Inconel 718 alloys	Alloys, Inconel 718 alloys	Short feed defect, warpage, part shifting defect	Powder layer optical image	94%, 96%, 94%	[65]
	LPBF	AlSi10Mg, bronze, Inconel 625, Inconel 718, stainless steel 316L, Ti-6Al-4V, Fe—3Si, stainless steel 17-4 PH	AlSi10Mg, bronze, Inconel 625, Inconel 718, stainless steel 316L, Ti-6Al-4V, Fe—3Si, stainless steel 17-4 PH	Recoater hopping, recoater streaking, debris, super-elevation, part failure, incomplete spreading	Powder bed image	97%	[66]
	LPBF	Inconel 718, stainless	Inconel 718, stainless	Overheating, normal, irregularity, balling	Optical image	99.7%	[67]
	DED	Stainless steel 316L, Ti-6Al-4V, Fe—3Si,	Stainless steel 316L, Ti-6Al-4V, Fe—3Si,	Distortion	Thermal image	24 nm (RMSE)	[68]
	LPBF	Stainless steel 17-4 PH	Stainless steel 17-4 PH	Defects from standard energy, low energy, high energy, very low energy	Powder layer images, part slice images after laser scanning	99.4%	[69]
	LBAM	Not mentioned	Not mentioned	Metal fracture, metallographic defects	Metal fracture microscope images, Metal metallographic images	82%, 87.5%	[70]
	LPBF	Ti-6Al-4V, CM247-LC	Ti-6Al-4V, CM247-LC	Porosity, surface imperfections	Acoustic spectroscopy, optical image	No specific accuracy	[71]
	LBAM	Ti-6Al-4V	Ti-6Al-4V	Laser additive manufacturing transvers and longitudinal, laser cladding	Microstructure	90.4%	[72]
	LPBF	H13 tool steel	H13 tool steel	Delamination, splatters, good quality	Thermographic off-axis imaging	96.80%	[73]
	LPBF	Stainless steel 316L	Stainless steel 316L	Poor, medium, high quality	AE signal	83%–89%	[74]
	DED	Ti-6Al-4V	Ti-6Al-4V	Porosity	Thermal image	92.07%	[75]

by mixing Ti-6Al-4V powder with H13 tool steel powder in the LMD printing process [35]. With the AE signal as the input data, this approach can detect two primary defects between crack and porosity. Moreover, Tapia et al. proposed a spatial Gaussian process regression model to learn and predict porosity for the SLM process [36]. Two printing parameters, laser power and scanning speed, which have the most significant effect on porosity formation, are fed into the Gaussian prediction model. The case study validated on 10 mm × 10 mm × 10 mm test coupons printed with 17-4 PH stainless steel powder. The result shows that the proposed model provided accurate porosity prediction under any printing parameters.

### 3.1.2. Traditional classifiers

Classification is a class of ML that focuses on predicting the label associated with a given piece of data. Sometimes classes are termed as labels, categories, or targets. Classification predictive modeling is the task of approximating a mapping function ( $f$ ) from input variables ( $X$ ) to discrete output variables ( $y$ ). In a classification task, the output can be a binary or multi-class classification according to the chosen classifier, such as good or bad quality, defect types.

Support vector machine (SVM) is a popular ML tool that offers a solution for both classification and regression. Various researchers have used this algorithm for defect detection; for example, Khanzadeh et al. applied multiple supervised learning methods (i.e., decision tree (DT), K-nearest neighbor (KNN), SVM, linear discriminant analysis (LDA), and quadratic discriminant analysis (QDA)) to predict porosity on the single track thin wall specimens (Ti-6Al-4V) by using melt pool thermal images [38]. In the SVM method, when selecting the polynomial as the kernel function, the porosity prediction accuracy is 97.97%. Fig. 8 shows the overall SVM methodology for porosity prediction. To classify the melt pool morphologies, Scime et al. developed a flaw formation identification method for the LPBF process with a multi-class SVM, which can

detect five melt pool types on a 10 mm × 20 mm rectangle made with Inconel 718 powder: under-melting, balling, spatter, porosity, and desirable [40]. Gobert et al. applied SVM to detect defects on a staircase cylinder fabricated with stainless steel GP-1 powder in the LPBF process [44]. By labeling different flaws (i.e., porosity, incomplete fusion, crack, or inclusions) with computer tomography (CT), the properly trained model achieved an over 80% defect detection accuracy. The flaw with a diameter larger than 47 µm can be identified. Petrich et al. developed an approach based on the SVM and neural networks to detect defects during the LPBF process with high-resolution layer-wise images [41]. By utilizing a cross-validation methodology, the proposed algorithm in situ anomaly detection achieved a 90% accuracy for a staircase cylinder made with stainless steel GP-1 powder. Imani et al. investigated the printing process to figure out the effects different printing process conditions had on fusion porosity in LPBF [42]. By analyzing the in-process layer-by-layer optical images, the result shows the process conditions significantly impact the porosity generation. This approach satisfies statistical fidelity by linking the features extracted from the layer-by-layer images to the process condition with ML methods. Several ML classifiers (SVM, complex tree, LDA, KNN, bagged trees, and feed-forward neural network) are applied in this research. The SVM classifier achieved an 89.36% porosity detection accuracy with F-score for the cylinders of 10 mm diameter × 25 mm height manufactured with Ti-6Al-4V. The resolution for the pore detection is larger than 65 µm. Mahmoudi et al. built an anomaly detection system for the LPBF printing process [34]. This system detects printing process deviations by using the thermal signals obtained from the thermal images of the melt pool. Classifiers, including logistic regression (LR), KNN, SVM, and random forests (RF), are utilized to decide whether the printing process is in control or out of control through a step-by-step process. The result shows this framework had a very low error rate for cavity defect detection.

SVM is also utilized by researchers for product quality prediction and

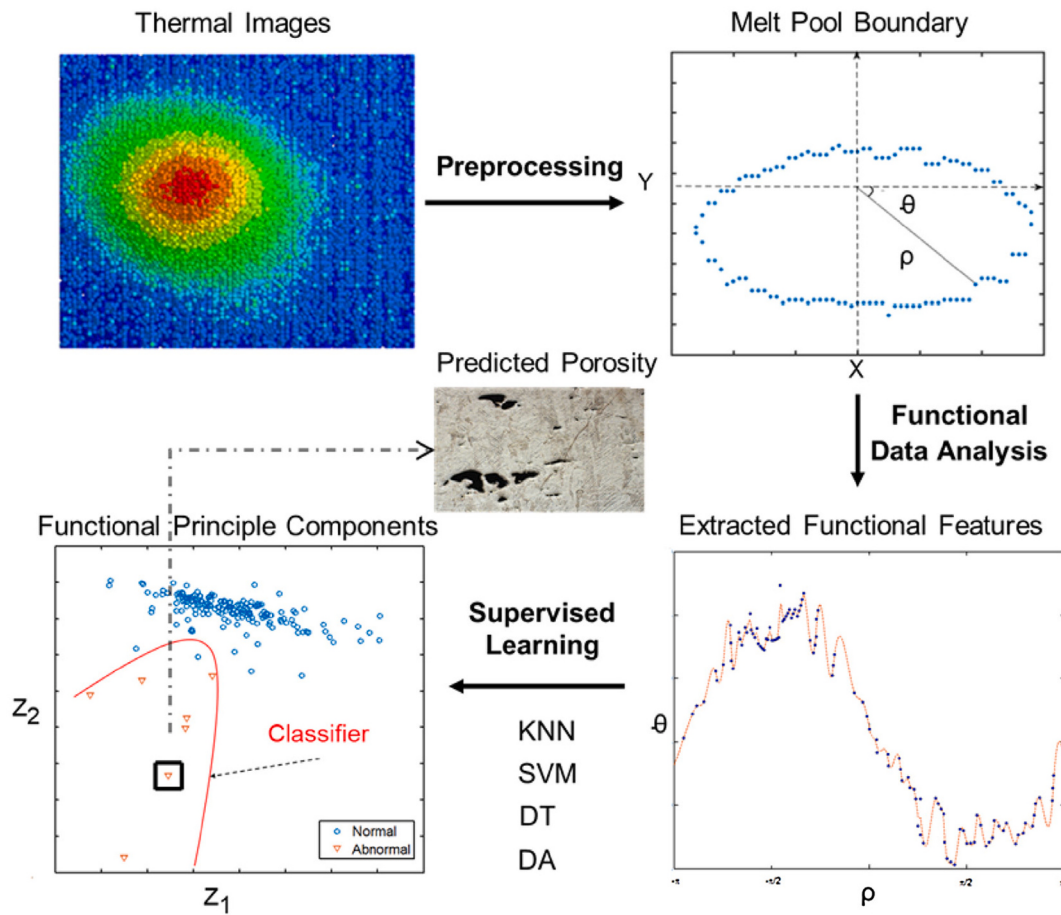


Fig. 8. Demonstration of porosity prediction procedure using supervised machine learning [38].

inspection. Seifi et al. proposed a method to detect product anomalies in real-time for LBAM and verified on the DED printing process [39]. After extracting the key layer-wise signature features from the melt pool images with multilinear principal component analysis (MPCA), an SVM classifier is used to extract key layer-wise signature features to predict the product's quality. The proposed methodology prediction accuracy obtained an F1-score of 91.65% and was validated on a thin wall fabricated with Ti-6AL-4V. Lu et al. utilized the least square support vector machine (LS-SVM) to predict the track's depositing height for the DED process [45]. With laser scanning speed, laser power, and powder feeding speed as inputs, this model provided knowledge on the whole printing part's precision. The experimental result on a thin wall printed with AISI316L powder shows that the LS-SVM algorithm prediction value had a high correlation coefficient with the experimental value of 0.971. Ye et al. proposed a defect-recognition approach for the LPBF process [37]. Using SVM and extracted features from recorded acoustic signals, this method achieved accurate diagnosis for five different melted states (i.e., overheating, medium overheating, underheating, medium underheating, and normal) for the single tracks printed by 304L stainless steel powder.

The Bayesian classifier is a probabilistic classifier that gives probability information about the examined product layer being defective, which could also be considered a product quality quantitative method. Therefore, the Bayesian classifier is also a useful tool for defect detection in the LBAM processes. A Bayesian classifier was built and trained by Aminzadeh et al. to classify the product quality fabricated by Inconel 625, which can detect the defective regions or abnormal layers in LPBF [46]. The training data is labeled printing process images with detailed layer defects and porosity. The result shows that with appropriate feature selection, the defect identification performance is 89.5%. To

predict the product quality (stainless steel 316L powder) printed by LPBF, Hertleina et al. proposed a Bayesian network, which combines the printing process parameters with product quality characteristics [76]. After training, the forecasted mean of a printed product quality characteristic (hardness) is within 0.41 standard deviations of the true value. Bartlett et al. utilized a three-dimensional digital image correlation system to predict microstructural defects (i.e., lack of fusion and keyhole) from AlSi10Mg aluminum powder bed quality in direct metal laser sintering (DMLS) printing process [47]. By feeding the powder anomaly topology images into the Naïve-Bayes classifier, the algorithm can predict microstructural defect formation probability according to the in-process powder bed error. The defect and no defect prediction accuracy for three energy density printing conditions (i.e., low, standard, and high) are 66%, 77%, and 72%, respectively.

In addition, other classifiers are also utilized by researchers for detecting defects in the LBAM processes. For example, Montazeri et al. presented an in-process porosity monitoring approach using optical emission spectroscopy [48]. The experimental result shows that using the graph Fourier transform coefficients as the input feature within the KNN model had the best layer porosity-level prediction accuracy for two-level classification (90% F-score) on the disk manufactured with nickel alloy 718 powder. In addition, the computation time only needs less than 0.5 s. Chen et al. proposed a rapid surface defect detection method for the DED technology, which integrates the in situ point cloud processing with ML [49]. The algorithm used in this research combined unsupervised with supervised ML to identify and classify the surface defect. The unsupervised algorithm is used to segregate the potential surface defect region from the point cloud. This approach registered the defect's existence and typed recognition by inputting the clustering result from an unsupervised algorithm into the supervised algorithm.

The surface defects are categorized into four classes: no defect, bulge defect, dent defect, and wavy defect. To compare the classification accuracy, eight algorithms are applied; the most accurate algorithm for classification is the KNN classifier, with an accuracy of 93.15%. Garcia-Moreno et al. presented an image-based porosity classification method by utilizing a random forest algorithm for the LMD printing process [50]. The random decision tree classifier achieved an accuracy of 96.45%, 94.56%, and 92.21% for the macropores, micropores, and elongated pores on the dogbone sample fabricated with Al-5083 powder, respectively. The proposed method can segment and classify pores between 5 and 250  $\mu\text{m}$ .

### 3.1.3. Artificial neural network

Artificial neural networks (ANN) are a class of ML algorithms modeled loosely after the human brain and designed to recognize patterns. A typical ANN usually has three parts: the input layer (first layer), one or more hidden layers (middle layers), and the output layer (last layer). Each layer consists of a collection of neurons, which are nodes connected with the other nodes via links (also termed synapse). Each link has a weight, which decides one node's impacting strength to another node. During the training process, the ANN model forms probability-weighted associations between the input and target. The target output is given; thus, training is performed by reducing the

difference between the network's processed output and the target output. Backpropagation is used to adjust the model's weights and biases, given the change of error at each step (also termed the gradient) and a predefined set of learning rules. After successive and sufficient adjustments, the network's output is increasingly similar to the target output, which means the network has been fully trained and can be used for future prediction.

When fed a labeled dataset for training, the ANN is helpful for clustering and classification. Petrich et al. developed an approach based on the ANN to detect defects during LPBF with high-resolution layer-wise images [41]. By utilizing cross-validation strategies for training and testing, close to 90% accuracy is achieved when using the ANN model to detect the defect for a staircase cylinder fabricated by stainless steel GP-1 powder. Gaja et al. used an ANN model to detect product defects in the LMD printing process [35]. With the AE signal as the input data, this approach can detect crack and porosity simulated by mixing Ti-6Al-4V powder with H13 tool steel powder. To predict the product surface texture in LPBF, Ozel et al. applied several ML algorithms to establish the relationship between printing process parameters (i.e., laser energy density and scan strategy) and measured surface texture parameters [51]. For the ANN algorithm, it is able to reflect the actual conditions when the measurement data is sufficient; for the genetic programming (GP), it is good at selecting the best LPBF process parameters for the

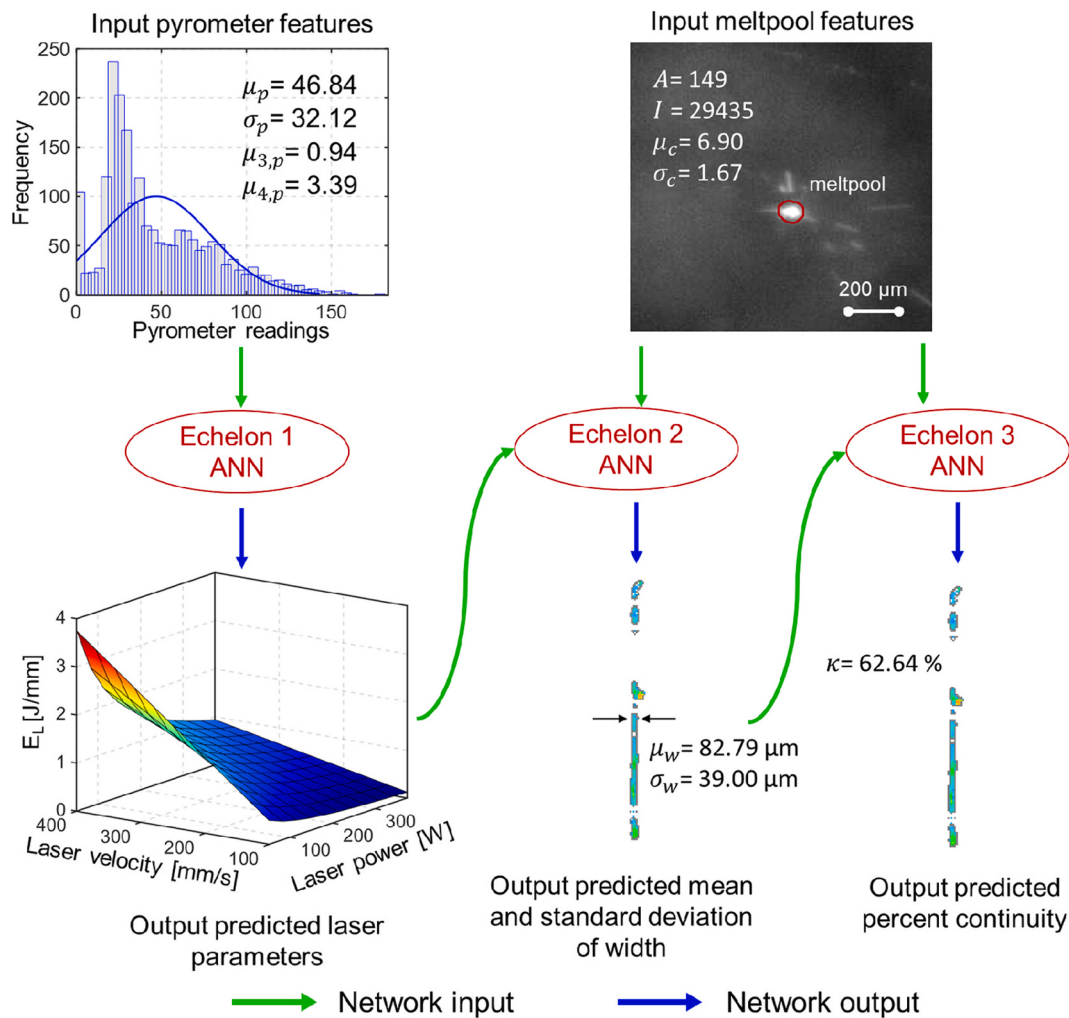


**Fig. 9.** A schematic of the sequential decision analysis neural network (SeDANN). The sensor data and height map shown above belong to a single-track deposited at linear energy density (EL) of 0.33 (i.e., balling regime). The statistical probability distribution features extracted from the pyrometer are used in the first echelon ANN to predict the laser process parameters (P and V) followed by melt pool features derived from the high-speed video camera to predict the mean width and standard deviation and single-track continuity at higher echelons [52].

cubes fabricated with nickel alloy 625 with the dimension of 16 mm × 16 mm × 15 mm. Gaikwad et al. developed and evaluated an ML-based quality assessment model for a single track printed with stainless steel 316L powder by LPBF process [52]. The study researched various printing parameters (i.e., laser power and laser velocity) effects on single-track's quality and analyzed the quality measurement with height-map by using the extracted mean and standard deviation of width and percent continuity. The experimental result shows that the proposed sequential decision analysis neural network (SeDANN), which uses the sensor data-derived features, performs better than the other ML models, such as long short-term memory recurrent neural network (LSTM-RNN), in speed and accuracy for balling, lack-of-fusion, conduction, and keyhole detection. Fig. 9 shows the schematic of the SeDANN proposed by Gaikwad et al.

A deep neural network (DNN) is an ANN with multiple layers between the input and output layers. The DNN algorithm finds suitable mathematical manipulation to exploit the input information into the output, whether it is a non-linear or linear relationship. DNNs have also been applied to defect detection in the LBAM processes. For example, Imani et al. designed a DNN model for real-time incipient geometry defects detection from the spatial characterization images in the LPBF process [53]. The experimental result shows that the proposed DNN model effectively achieved geometry flaw detection on drag link joint object (23.7 mm × 13.3 mm × 27.3 mm). The accuracy achieved is 92.5% for the 750 µm cylinder and cube defect. As laser power has a huge impact on the pores and cracks formation, which directly determines the printing product quality, Kwon et al. applied a DNN in LPBF to find the link between melt-pool images and laser power [77]. The cuboid product with a dimension of 8.5 mm × 8.5 mm × 4 mm is fabricated with stainless steel 316L. The proposed DNN model's classification accuracy on this product is 98.9%, which is helpful for understanding the product microstructure formation by abnormal laser power. Mohammadi et al. presented a novel approach for defect detection in the LPBF process by utilizing the elastic waves from the AE sensor [78]. The proposed approach can detect three types of defect (i.e., parts with minimum defects, parts that had only intentional cracks, and parts that had both intentional cracks and porosities) on the cylindrical parts with a dimension of 20 mm diameter and 10 mm height fabricated with H13 tool steel powder. Three ML algorithms are utilized to analyze and interpret the data. Firstly, a K-means clustering is applied for data labeling, then followed by a DNN to match the AE signal with the correct

defect type. Secondly, a PCA is employed to reduce the data's dimensionality. A Gaussian Mixture Model (GMM) is utilized to accelerate the defect detection speed. Thirdly, a variational auto-encoder method is applied to get a general feature of the AE signal that could be an input for the classifier. The unique contribution of this work is that the proposed approach can generalize the classifier to be used for different materials without the need for training.

### 3.1.4. Convolutional neural network

A convolutional neural network (CNN) is a class of ANN that incorporates one or more convolutional layers into the architecture of the neural network for feature extracting, one or more pooling layers for subsampling, and then with one or more fully connected layers for the output. CNN is the most popular deep learning (DL) algorithm for image recognition, image classification, and object detection due to its outstanding image processing and pattern recognition performance.

The CNN algorithm has been used for defect detection in the LBAM process. For example, Scime et al. utilized a CNN algorithm for autonomous anomaly detection and classification in LPBF [66]. The proposed model achieved six types of flaws detection (i.e., recoater hopping, recoater streaking, debris, super-elevation, part failure, incomplete spreading) with an overall accuracy of 97%. A case study validated the proposed algorithm's ability by printing a heat exchanger model with Inconel 718 powder. Fig. 10 shows the flowchart of the ML technology, which is utilized by Scime et al. for defect detection. Baumgartl et al. developed a printing defect detection system by combining thermographic off-axis images with a DL-based CNN [73]. By using the depthwise-separable convolutions to reduce the dimension of channels into the neural network architecture, this technique achieved an accuracy of 96.80% for delamination and splatter defects. Furthermore, the model's architecture is small and therefore has reduced computational cost, which shows great potential to apply the proposed algorithms for online defect detection. Cui et al. utilized a CNN algorithm to inspect the defect for the product produced by LMD [55]. The materials in this research include AISI 304 stainless steel, AISI 316 stainless steel, Ti-6Al-4V, AlCoCrFeNi alloys, and Inconel 718 alloys. The proposed algorithm had an accuracy of 92.1% for defects, such as gas porosity, crack, and lack of fusion. Zhang et al. described a porosity prediction CNN model for the LBAM process [61]. With the melt pool image from the single track manufactured by sponge titanium powder, the algorithm had a 91.2% porosity detection accuracy and is able to predict the micro-pores

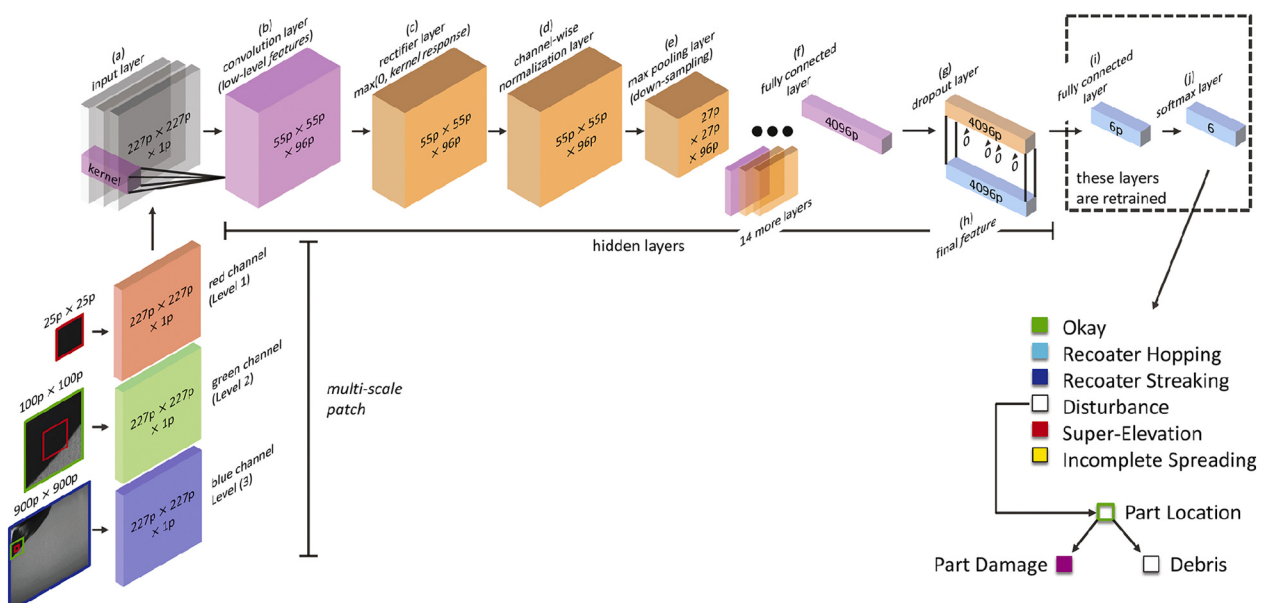


**Fig. 10.** Flowchart of the implementation of the multi-scale CNN ML technique [66].

below 100  $\mu\text{m}$ . Moreover, Guo et al. presented a physical-driven CNN model to predict porosity on thin-wall structure from Ti-6Al-4V powder by using metal pool thermal images obtained from a pyrometer for the DED process [62]. When combining the data-driven feature from the pyrometer image with the physical feature from finite element analysis, the proposed algorithm had a reported 100% porosity prediction accuracy. Zhang et al. proposed an online monitoring method for LBAM products, which relies on a CNN algorithm [59]. The experiment results show that when using a small local image block, the classification accuracy for bonding quality (i.e., under-melt, normal, and over-melt) is 82%; when utilizing the full images, the model accuracy was reported as 100%.

Product quality guarantee can also be achieved with CNN algorithms for the LBAM processes. Yuan et al. built a CNN model to monitor the LPBF printing process by analyzing the single track quality made with 316L stainless steel [58]. After training with the frames obtained from the melt pool video, this model is able to predict the track width, width standard deviations, and track continuity. Zhang et al. utilized CNN for product quality level identification in the LPBF process [43]. The input data is melt pool, plume, and spatter images obtained by a high-speed camera from the 8 mm single track printing process with stainless steel 316L powder. The proposed CNN model's quality level identification accuracy is 92.7%. Furthermore, one image identification only takes 8.01 milliseconds. A CNN-based approach was proposed by Gaikwad et al. to monitor and predict the thin-wall build quality with Ti-6Al-4V in LPBF [56]. After training with the layer-wise thin-wall optical images captured by an optical camera in the LPBF printer, the model can predict the X-ray computed tomography (XCT) derived statistical quality features, such as thickness and edge consistency, with an accuracy exceeding 85%. Kunkel et al. proposed a product quality assurance method for LBPF by utilizing a CNN-based image classification algorithm [57]. This CNN method had a promising quality identification accuracy of 98.9% for the product made with AlSi10Mg powder. Li et al. proposed a DL-based process monitoring for the DED technology [63]. The proposed CNN model used thermal images from the straight stick part manufactured with 0Cr18Ni9 powder as input, which had an accuracy of over 80% for different printing condition recognition (i.e., normal, lower power, low and high speed).

Deep convolutional neural network (DCNN) algorithm is a subclass of CNN, and therefore ANN, that utilizes more layers in the architecture. A DCNN is defined as one that utilizes at least 20 layers in its formulation in this work. There are several specific models for DCNNs with distinct structures, such as GoogleNet (also called InceptionNet), VGGNet, and ResNet. Generally, DCNN is better suited at detecting non-linear relationship and feature extraction than traditional CNN but require more data and longer training time than their more-traditional counterparts. Due to their capability to detect non-linear patterns, DCNN algorithms have been widely applied to detect defects in LBAM. Han et al. exploited defect detection in LBAM by utilizing a DCNN (Inception-v4) to analyze and classify images from the manufacturing process [70]. In this research, the DCNN model was applied to two datasets, metal fracture microscopic images and product parts of metal metallographic images. For the metal fracture microscopic image dataset, the model achieved an accuracy of 82%, recall of 93.8%, and precision of 96.8%; the model trained on the metal metallographic images, the accuracy, recall, and precision is 87.5%, 96.3%, and 97.6%. Li et al. built a novel CNN model structure based on a dense convolutional network to recognize the microstructure in LBAM [72]. The result shows the accuracy is 90.4% and one microstructure image processing time only needs 0.1 s. Gonzalez-Val et al. proposed a novel ConvLBM (CNN for laser-based manufacturing) method to estimate dilution in the LMD process [60]. Dilution is an important quality indicator: a low dilution may produce insufficient bond and generate warping, but a high value means a large heat-affected zone, which has a high defect probability because of the thermal expansion [79]. ConvLBM is a modified CNN model based on ResNet [80] to extract key features from the raw medium wavelength

infrared coaxial images. The trained ConvLBM model estimated dilution with a root-mean-square error (RMSE) of 2.8%.

Ensembles of CNNs have also been developed to provide better fault detection capabilities than the traditional stand-alone CNNs. Shevchik et al. investigated combining spectral CNN with acoustic emission for quality monitoring in LBAM [74,81]. The classification confidence varies between 83% and 89% on a cuboid with a dimension of 10 mm  $\times$  10 mm  $\times$  20 mm manufactured with stainless steel 316L. Xiao et al. developed a two-stage convolutional neural network (TS-CNN) to predict different kinds of defects in LBAM [65]. The research demonstrated that this approach had high accuracy and efficiency in coping with geometrical distortion manufactured with pure polyamide (PA) and PA/TiO<sub>2</sub> composite. The respective prediction accuracy for the warpage, part shifting, and short feed defects is 94%, 96%, and 94%. Williams et al. developed a CNN model named Densely connected convolutional block architecture for multimodal image regression (DCB-MIR) to detect product defects in metal LBAM [71]. This proposed model utilized the printing product's SRAS (spatially resolved acoustic spectroscopy)-derived acoustic velocity maps as input data and decoded them to a resembling optical micrograph as output. The model had high defects detection accuracy (i.e., porosity and surface imperfections) for the titanium alloy and nickel alloy samples. The defects were not distinctly recognizable in the as-measured SRAS acoustic map and blurred in the optical image. Zhang et al. proposed a hybrid CNN to monitor the printing process in LPBF [67]. This hybrid CNN architecture consists of two CNN models; the first one is utilized to study the spatial features from a single printing process image and the second one is applied to product quality classification. The model's overall detection accuracy on the 10 mm single track manufactured with stainless steel 316L powder is up to 99.7% for the overheating, normal, irregularity, and balling defects. Scime et al. built a new dynamic segmentation CNN (DSCNN) model for real-time pixel-wise semantic segmentation with layer-wise powder bed images as input [64]. The proposed DSCNN model had a wide application range of powder-bed-based AM machines, spanning from LPBF, to electron beam PBF, to binder jetting. The model segmented and located the defect, include recoater hopping, recoater streaking, incomplete spreading, swelling, spatter, soot, debris, super-elevation, part damage, and porosity, with good accuracy. Yazdi et al. proposed a hybrid DL model to monitor the printing process parameters, which potentially affect the porosity defect production [54]. The input data is the statistical features extracted from powder bed images by wavelet transform and texture analysis. The proposed model had a 97.14% F-score porosity prediction accuracy on a cylinder (a height of 25 mm and a diameter of 20 mm) fabricated with titanium alloy and Ti-6Al-4V powder. By applying a bi-stream DCNN model, Caggiano et al. built an online defect recognition system for LBAM [69]. The pre-alloyed Inconel718 powder layer image and laser scanning layer image are input into an ML algorithm as training data to manifest the defect produced by improper process conditions. The study result shows that a mean defective condition-related image pattern recognition accuracy of 99.4% was achieved on the final disc with a 40 mm diameter and 20 mm height.

Novel ensembles of ML techniques integrate different algorithms together to enable the new one to take full advantage of the strengths from every integrated algorithm for detecting defects in LBAM, which researchers also utilize. For example, Francis et al. developed a novel DL approach named CAMP-BD (Convolutional and Artificial Neural Network for Additive Manufacturing Prediction using Big Data), which integrates CNN with an ANN algorithm for analyzing the thermal images. It used the relevant process/design parameters as input data to predict fabricated product distortion [68]. The whole CAMP-BD model is displayed in Fig. 11. The distortion prediction result on a disk (5 mm thick and 45 mm diameter) made with Ti-6Al-4V powder, shows that most of the predictions are within the metal LBAM machines' tolerance limits. The distortion prediction RMSE on training data is 24  $\mu\text{m}$ . Tian et al. developed a DL-based in situ porosity detection method for LBAM,

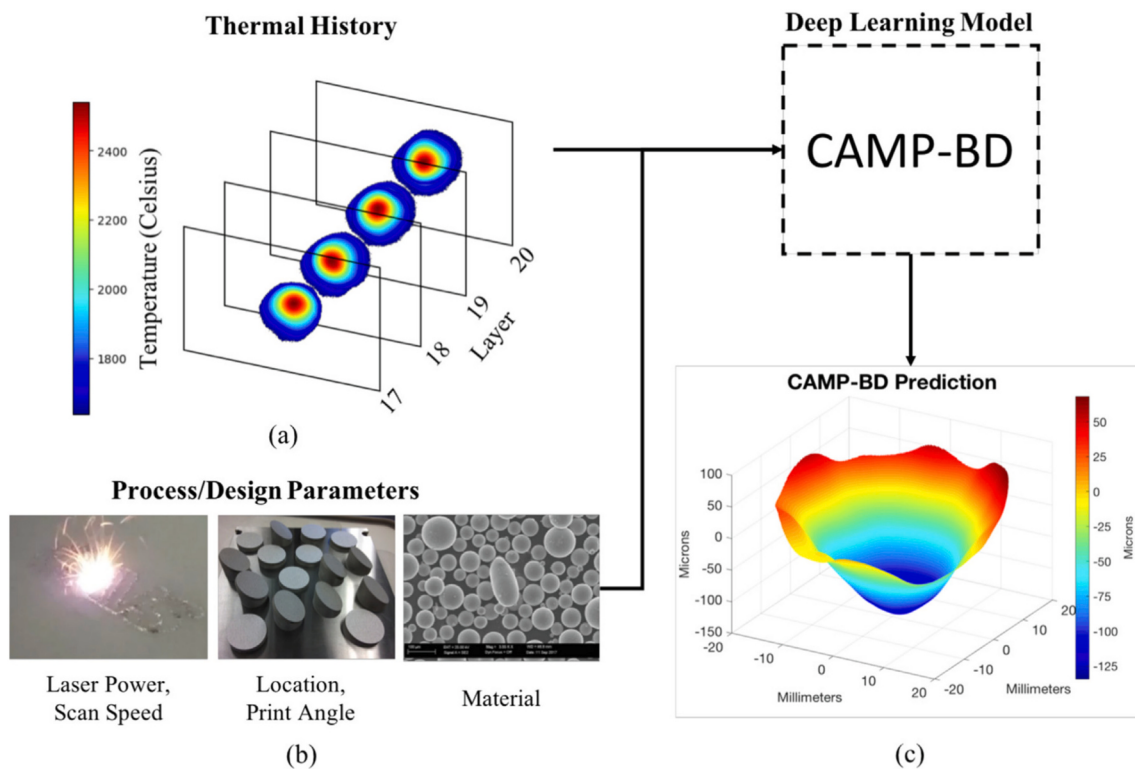


**Fig. 11.** Displaying the CAMP-BD model [68]: (a) the tensor structure of thermal history is visualized; (b) various process/design parameters are listed as examples of additional inputs to CAMP-BD; and (c) an example prediction of CAMP-BD.

which uses the melt pool thermal images to monitor the melt pool and predict porosity [75]. A PyroNet based on CNN and an IRNet based on long-term RNN two different algorithms are utilized to correct layer-wise porosity. For the PyroNet, the input is in-process images obtained from pyrometry, and for the IRNet, the input data is sequential thermal images captured from a thermal camera. To have a higher porosity prediction accuracy, two algorithms are fused together when making the final decision. The experimental result on a Ti-6Al-4V thin-wall

structure shows that the average porosity prediction accuracy on six-folds is 98.93%.

### 3.2. Unsupervised learning

Unsupervised learning is a category of ML that looks for formerly undetected patterns in a dataset without pre-existing targets or labels and only involves minimal human supervision. Compared with

**Table 2**  
Unsupervised ML algorithms utilized in defect detection for LBAM processes.

ML category	ML algorithm	AM technology	Material type	Defect type	Dataset type	Accuracy	Reference
Unsupervised learning	K-means clustering	LPBF	AlSi10Mg, bronze, Inconel 625, Inconel 718, stainless steel 316L, Ti-6Al-4V, Fe—3Si, stainless steel 17-4 PH	Recoater hopping, recoater streaking, debris, super-elevation, part failure, incomplete spreading	Powder bed image	98%	[82]
		LPBF	Ti-6Al-4V, Inconel 718, Ti-5553, Haynes 282	Key hole, lack of fusion	X-ray computed 3D pore tomography, 2D pore micrograph	No specific accuracy	[83]
		LPBF	Stainless steel 316L	Undesired overheating defect	Optical image	No specific accuracy	[84]
		LPBF	AlSi10Mg	Drift, no drift	Optical tomography image	No specific accuracy	[85]
		DED	Mixing Ti-6Al-4V with H13 tool steel	Crack, porosity	AE data	No specific accuracy	[86]
		DED	Ti-6Al-4V	Process condition variation	AE signal	87%	[87]
Deep belief network	DED	7075-Al alloy powder		Surface roughness porosity	Spectral	Refer to paper	[88]
	LPBF	Stainless steel 304		Balling, slight balling, normal, overheating, slight overheating	Acoustic signal	95.93%	[89]
Self-organized maps	LPBF	Stainless steel 304L		Over-melted, middle over-melted, normal-melted, middle under-melted, under-melted	NIR image	83.40%	[90]
	DED	Al-5083		Super-micropores, cracks, hybrid pores, inter-micropores defect	Optical microscope image	95%	[91]
	DED	Ti-6Al-4V		Porosity	Melt pool image	96%	[92]

supervised learning, which uses training data with labels, unsupervised learning, also termed self-organization, can model probability densities based on the input data. The advantage of unsupervised learning is that no labeled data is needed. Table 2 shows a list of unsupervised ML algorithms utilized for detecting defects in components manufactured using the LBAM processes, which contains key features of the reviewed research, including dataset type, material type, defect type, and algorithm performance.

### 3.2.1. K-means clustering algorithm

The K-means clustering (KMC) algorithm is one of the simplest yet most powerful unsupervised learning algorithms for solving clustering problems. The procedure follows a simple method to classify a given dataset through a pre-defined number of clusters (assume k clusters) fixed apriori. The main idea is to define k centers, one for each cluster. Scime et al. presented an approach for in situ monitoring and analysis of powder bed images, which shows promising potential to be used as a real-time control system in the LPBF process [82]. A computer vision algorithm is used in this approach for automatic defect detection and classification during the powder spreading process. Defect detection and classification are implemented by using a standard k-means unsupervised clustering algorithm to process the printing image. The final algorithm achieved six types of flaw detection (i.e., recoater hopping, recoater streaking, debris, super-elevation, part failure, and incomplete spreading). Snell et al. trialed an unsupervised ML method (KMC) for rapid pore classification in metal additive manufacturing [83]. In this research, the pore data was collected by two different techniques: 3D pore data from the XCT and 2D pore data from microscopy, with multiple alloy (Ti-6Al-4V, Inconel 718, Ti-5553, and Haynes 282). The result shows that KMC is suitable for 3D pores, it performs well both on lack-of-fusion pores and keyholes pores, but it cannot be used to analyze the 2D pore data. Grasso et al. developed an in-process defect spatial detection method by utilizing image data analysis for the LPBF process during the layer-wise printing process [84]. The proposed image KMC algorithm achieved defect detection automatically by detecting and positioning the potential defect in each layer. Taheri et al. developed an in situ process condition monitoring method for the DED process [87]. By utilizing the KMC to process the acoustic signatures from a single-layer (Ti-6Al-4V) printing process, the algorithm identified different process conditions (i.e., normal, low powder, and powder spray) with an accuracy of over 87%. In addition, Gaja et al. presented a novel real-time defect detection and classification system for the LMD process, which uses an acoustic emission sensor and a KMC unsupervised ML algorithm [86]. By analyzing the AE signal, the experimental result shows that the

KMC is able to recognize crack and porosity simulated by mixing Ti-6Al-4V powder with H13 tool steel powder, two different defects effectively. Ren et al. built an unsupervised model for product quality recognition manufactured by DED [88]. The proposed model has an LSTM-based autoencoder for extracting encoded features which contain information to express the original spectra. Then the extracted features are utilized to K-means clustering for product quality classification. Four 40 mm tracks with Al7075 alloy are printed in the research, and the result shows that the classification matches with the real track quality.

### 3.2.2. Deep belief network

A deep belief network (DBN) is a generative graphical model, or alternatively a class of deep neural networks, which is composed of multiple latent variable layers, and each layer is connected, but the units within each layer are not related. DBN is another useful ML algorithm, which has been utilized for defect detection in LBAM. Ye et al. demonstrated that acoustic signals are feasible for product quality monitoring, and DBN algorithms achieved a high defect detection rate among five melted states on single tracks manufactured with 304 stainless steel powder (i.e., balling, slight balling, normal, slight overheating, and overheating) without signal preprocessing [89]. Fig. 12 displays a generic classification-based DBN architecture that can be used for defect recognition with the acoustic signals from the LBAM printing process. As the plume and spatter signatures have a very close relationship with the melted state and laser energy density. Ye et al. applied DBN to the plume and spatter NIR images obtained from the LBAM printing process, and this approach achieved an 83.4% classification rate for over-melted, middle over-melted, normal, middle under-melted, and under-melted melted states on single tracks produced with 304 stainless steel powder [90].

### 3.2.3. Self-organized maps algorithm

Self-organized maps are a type of ANN trained by unsupervised learning to output a low-dimensional (generally two-dimensional), discretized representation of the input space of the training samples. As an effective dimensionality reduction method, self-organized maps are also applied to defect detection. Garcia-Moreno proposed an automatic porosity quantification method by utilizing an unsupervised ML classifier for the LMD printing process [91]. The final classifier based on self-organized maps obtained a 95% accuracy for the super-micropores, cracks, hybrid pores, and inter-micropores defect for the product manufactured with Al-5083 powders. The proposed algorithm is sensitive detecting the average size of 6.33  $\mu\text{m}$  inter-micropores. Moreover, Khanzadeh et al. proposed an in situ porosity prediction method for the

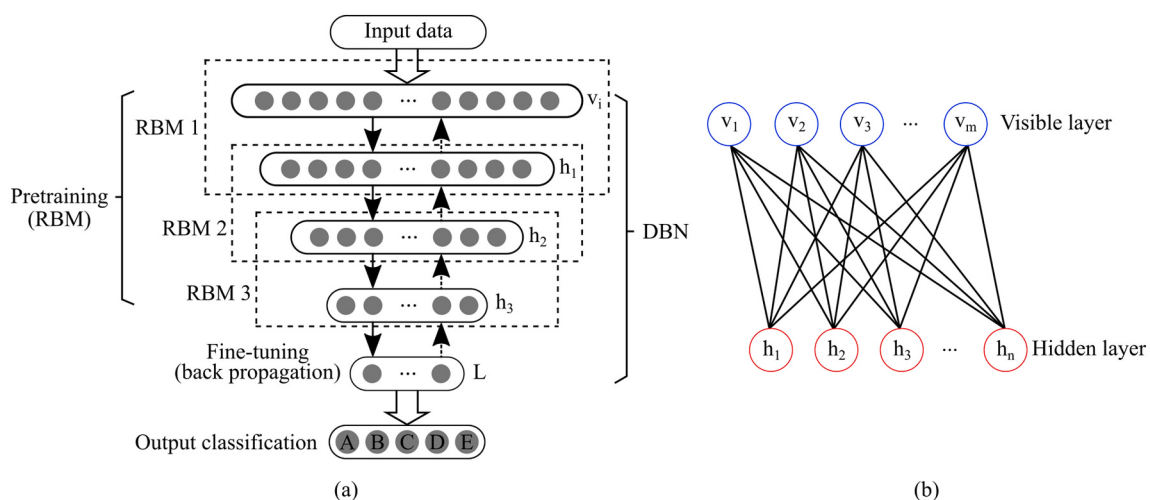


**Fig. 12.** An illustration of a generic classification-based deep belief network (DBN) with stacked RBMs (restricted Boltzmann machines): (a) deep belief network (DBN); and (b) restricted Boltzmann machine (RBMs).

DED process based on the printing melt pool images [92]. According to the melt pool's temperature distribution, the proposed self-organized maps model predicted the porosity position on a Ti-6Al-4V thin-wall specimen with an accuracy of 96%.

### 3.3. Semi-supervised learning

As discussed before, supervised learning uses a dataset that includes labels to train the algorithm to understand which features are important to the problem at hand. However, the generation of labeled datasets is a costly process, especially when dealing with large volumes of data. On the other hand, unsupervised learning is trained on unlabeled data and must identify features and determine their importance by themselves based on inherent data patterns. The disadvantage of any unsupervised learning is the limited application range. To counter these disadvantages, the concept of semi-supervised learning was introduced. In semi-supervised learning, the algorithm is trained upon a combination of labeled and unlabeled data. Typically, this combination contains a limited amount of labeled data and a larger amount of unlabeled data. This is helpful for a few reasons. First, the process of labeling massive amounts of data for supervised learning is often prohibitively time-consuming and expensive; however, a small amount of labeled data can significantly improve the learning accuracy when paired with a large volume of unlabeled data. Furthermore, too much labeling can impose human biases on the model. That means including lots of unlabeled data during the training process tends to improve the final model's accuracy while reducing the time and cost spent building it. In such conditions, semi-supervised learning can be of great practical value. In the research situation, as shown in Table 3, semi-supervised learning is also helpful as there is no need to label all data for training, which saves time and effort.

Semi-supervised ML has been studied by researchers for defect detection. Okaroa et al. introduced a semi-supervised ML algorithm for automatic defect detection in the LBAM printing process [93]. The result on the tensile test bars manufactured with Inconel 718 shows that the semi-supervised ML algorithm is a promising method for automatically identifying the LBAM product defects, which achieved a comparable result to a benchmark where all training data are labeled. To detect the inline drift in the LPBF process, Yadav et al. proposed a semi-supervised method, which uses certified product computer tomography as input data [85]. The supervised ML-based KNN algorithm is trained with the labeled input data from the unsupervised ML K-means clustering algorithm. Based on the case studies validated on cylindrical samples (diameter of 10 mm and height of 15 mm) with AlSi10Mg powder, the proposed semi-supervised ML algorithm had a reported 100% accuracy in predicting the exact drift layers.

Semi-supervised CNNs eliminate the challenges of collecting large labeling datasets, making them more efficient for detecting defects in the LBAM processes. Yuan et al. developed a semi-supervised CNN, which only uses a limited amount of labeled data and a large amount of unlabeled data to monitor the LPBF printing process [94]. This approach used the videos from the single-track printing process with 316L stainless steel powder as input data. The result shows that the semi-supervised approach performs better than the fully supervised

approach, no matter whether it is a regression or classification problem. The semi-supervised CNN model's architecture used in this research is shown in Fig. 13. Li et al. proposed a DCNN model to analyze the product quality for the metal LBAM printing process [95]. In this method, the semi-supervised training data was used to mitigate the demand for a large amount of labeled image data. The algorithm proposed in this research had a 100% accuracy identification performance for under-melt, normal, and over-melt on the product made with ASTM F75 I CoCrMo powder.

### 3.4. Reinforcement learning

Reinforcement learning (RL) is one of the three basic ML paradigms, alongside supervised learning and unsupervised learning. It is an area of ML, which is concerned with how agents ought to take actions in a specific environment to get the maximum cumulative reward. Therefore, RL also has been used as an approach for defect detection in LBAM, as shown in Table 4. For example, Wasmer et al. integrated RL with acoustic data obtained from the printing process by acoustic emission to build quality monitoring in LBAM [96]. The classification accuracy obtained from a cuboid shape manufactured with stainless steel 316L shows that this RL approach had a high potential to be conducted in situ and in real-time. Furthermore, Yao et al. proposed a sensor-based product quality control model for the LBAM process through the constrained Markov decision process [97]. The experimental result shows that the proposed constrained Markov decision process provided an efficient policy for taking the right actions to remedy and mitigate incipient defects before the whole part is completed. Fig. 14 shows the flow diagram of the in situ control sequential decision-making framework for the LBAM process through the constrained Markov decision process.

## 4. Outlook

An appropriate and effective defect detection system is a key driver for the development of next-generation technologies in LBAM. Their implementation will continue to increase the quality, efficiency, consistency, and sustainability of metal components manufactured using the LBAM processes [98,99]. Future development for LBAM defect detection will likely be in the following four areas.

- 1) Integration of defect detection and product quality: The ultimate goal is to ensure the final product quality regardless of which algorithm is utilized for defect detection. In other words, the defect-to-property is the core for defect detection in LBAM. The defect detection should focus on detecting and evaluating the defect impact rather than just finding the defect. The decision-making system is also a critical part after defect impacting evaluation. Based on the evaluation result, the impacting defect level can be divided into negligible, marginal, and impactful. The printing process needs to be canceled to save energy, material, and time when an impactful defect occurs. For the decision-making system, the decision boundary from the machine learning algorithm has promising potential when combined with the defect impacting together.

**Table 3**  
Semi-supervised ML algorithms utilized in defect detection for LBAM processes.

ML categories	ML algorithm	AM technology	Material type	Defect type	Dataset type	Accuracy	Reference
Semi-supervised machine learning	K-nearest neighbors and K-means clustering combination	DED	AlSi10Mg	Drift, no-drift	Optical tomography image	No specific accuracy	[85]
	Gaussian Mixture model	LPBF	Inconel 718	Faulty, acceptable	Photodiode data	77%	[93]
	Semi-supervised convolutional neural network	DED	Stainless steel 316L	Track average width, track continuity	Video data	No specific accuracy	[94]
		LBAM	ASTM F75 I CoCrMo	Under-melt, beautiful-weld, over-melt	Micrograph image	90%	[95]

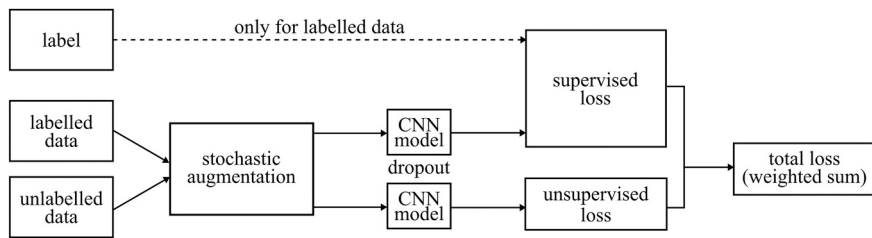


Fig. 13. Semi-supervised CNN architecture.

Table 4

Reinforcement learning algorithms utilized in defect detection for LBAM processes.

ML categories	ML algorithm	AM technology	Material type	Defect type	Dataset type	Accuracy	Reference
Reinforcement learning	Markov decision process	LBAM	Stainless steel 316L	Poor, medium, high quality	AE signal	74%, 79%, 82%	[96]
	Constrained Markov decision process	LBAM	Not mentioned	Defect states	Optical image	No specific accuracy	[97]

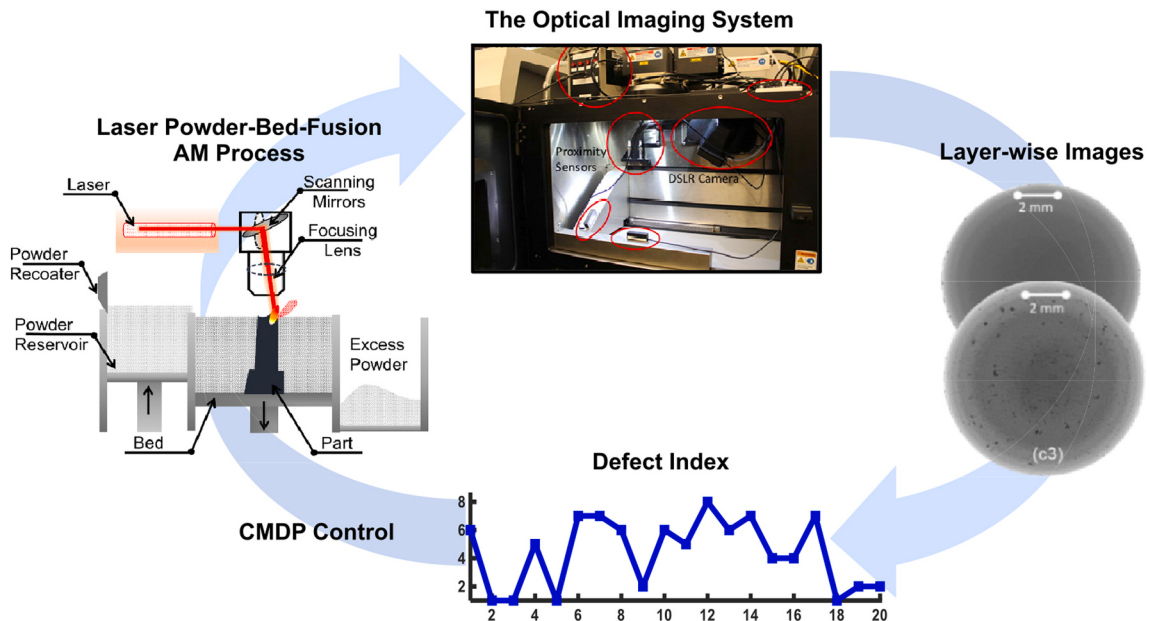


Fig. 14. Flow diagram of the sequential framework of constrained Markov decision process to control the quality of LBAM builds [97].

- 2) Data fusion and advanced algorithms: Signals from the different processes vary significantly in terms of temporal and spatial resolution. Sensors with different accuracies and resolutions need to be synchronized to handle different characteristics of the signal features, which provide a holistic understanding of the printing process. The improvement for the future advanced algorithms has two sides. (1) Fusion algorithms include in-process signal processing and defect detection. Most of the existing machine learning algorithms can only handle one type of input data. However, the defect has many influence factors and performance characteristics. Just detecting defects from only one dimension is not comprehensive and accurate. The advanced algorithm should have the ability to handle multi-type input at the same time. Hybrid machine learning and deep learning will play an increasingly important role in this field. (2) The development of the latest algorithms and their application. Hundreds and thousands of new algorithms are developed nowadays with new features and abilities. This development will significantly broaden the defect detection perspective in LBAM. For example, physics-

informed ML will enable the integration of most recent understanding of defect formation mechanisms to reduce the data requirement and increase the detection accuracy [100].

- 3) Real-time feedback control and correction system that couples sensor data, computational models with advanced algorithms: The ways to mitigate the defects impacting can be done by correcting them when the defects are initially detected or when the defects are predicted before they occur. Therefore, real-time feedback control and correction systems and the predictive capability of the algorithms are essential, which should fuse various sensor data, computational models with advanced algorithms together to achieve this goal. Reconstruct 3D objects by the machine learning algorithm based on the different input signals, where physics-based computational models can supplement the experimental data with future status. Then mapping the detected or predicted defects to the printing code. According to the defect information, correct the correspondent code (e.g., laser speed, laser power, and the axis movement) to mitigate the next printing flaws. This may be a feasible way, which has been

proven on the other printing technology [101]. In the foreseeable future, the LBAM system will be more widely applied by adding an effective defect detection and feedback system to mitigate printing flaws [102,103].

- 4) More compatible system: Active work has been performed in defect detection for LBAM; however, the algorithm is mostly specific to one defect and limited to one specific printer. As the development of a new detection system for another printing technology or another printer, even another material is time and effort consuming. Thus, a more unified and compatible framework that flexibly integrates available sensors, algorithms, and computational modeling can be transferred to the other system is important, which certainly will accelerate technology advancement. For example, transfer learning [104], which can boost the speed and accuracy of the training process, will play a significant role in compatible system development.

## 5. Conclusion

This paper summarizes recent research focused on the machine learning (ML) algorithms used in defect detection systems for the metal laser-based additive manufacturing (LBAM) processes. The comprehensive and exhaustive information listed in the paper provides a reference to help readers choose a suitable ML algorithm for detecting defects based on different printing technologies, material types, defect types, and data types.

Choosing a suitable ML algorithm is critical to achieving the appropriate level of defect detection in any LBAM system. A summary of commonly chosen ML algorithms is presented in this work. Convolutional neural networks (CNN) are the first choice when dealing with image data due to their unique advantages of processing image features. Using powder bed images, product layerwise optical images, or melt pool images, CNNs can be utilized for detecting various defects or product quality levels. Support vector machines using the alternative kernel function are a good choice for classification and are capable of handling both sensor signal and image data to perform both binary and multi-class classification. K-means clustering is a widely utilized algorithm in unsupervised and semi-supervised ML to partition the observations into different defect clusters. The Markov decision process is the most common algorithm for reinforcement learning, which performs well on both sensor signal and image data to detect defects and to evaluate product quality.

From the listed algorithms utilized in defect detection for LBAM processes, supervised machine learning algorithms are the most common. However, as supervised machine learning requires that all data be labeled it is time and effort-consuming. Algorithms that leverage unsupervised and semi-supervised learning have started to gain traction in the field and have demonstrated great potential to expand the field of fault detection in LBAM processes. Moreover, reinforcement learning is also being explored for defect detection in the LBAM process and offers the potential to develop accurate and highly efficient fault detection models.

While machine learning has its unique advantages; the application prerequisite is rigid. The small databases typically available for manufacturing systems usually results in over fit models that lead to poor fault detection accuracy. A considerable barrier for the real-world adoption of machine learning in defect detection of LBAM is the lack of a comprehensive, precise, and accessible databases for different materials, designs, and printing processes. A solution to this challenge is the development of a standard database with uniform design and fault criteria. Such a database would provide a large volume of accessible data for researchers. By leveraging transfer learning off of a massive database, reliable fault detection methodologies could be developed without the need of generating large specific datasets for each part or process.

It is worth pointing out the disproportionality in machine learning approaches for LBAM defect detection. Most of the literature's machine learning applications focus on directed energy deposition and laser

powder bed fusion; no research has been done on laser-based wire-feed systems.

## Declaration of competing interest

The authors declare that they have no known competing financial interests or personal relationships that could have appeared to influence the work reported in this paper.

## Acknowledgements

This material is based upon work supported by the South Carolina Research Authority under grant 30228 and the South Carolina Space Grant Consortium under grant 521179-RP-SC007. The support of these agencies is gratefully acknowledged. Any opinions, findings, and conclusions, or recommendations expressed in this material are those of the authors and do not necessarily reflect the views of the South Carolina Research Authority or the South Carolina Space Grant Consortium. Distribution Statement A. Approved for public release: distribution unlimited.

## References

- [1] Jiang Jingchao, Xiong Yi, Zhang Zhiyuan, Rosen David W. Machine learning integrated design for additive manufacturing. *J Intell Manuf* 2020;1–14.
- [2] Jiang Jingchao, Newman Stephen T, Zhong Ray Y. A review of multiple degrees of freedom for additive manufacturing machines. *Int J Comput Integr Manuf* 2021;34(2):195–211.
- [3] Singh Sunpreet, Singh Gurminder, Prakash Chander, Ramakrishna Seeram. Current status and future directions of fused filament fabrication. *J Manuf Process* 2020;55:288–306.
- [4] Gisario Annamaria, Kazarian Michele, Martina Filomeno, Mehrpouya Mehrshad. Metal additive manufacturing in the commercial aviation industry: a review. *J Manuf Syst* 2019;53:124–49.
- [5] Wohlers TT. Wohlers report 2021: 3D printing and additive manufacturing state of the industry. Wohlers Associates; 2021.
- [6] Tarasankar DebRoy HL, Wei JSZuback, Mukherjee T, Elmer JW, Milewski JO, de Allison Michelle Beese A, Wilson-Heid AD, Zhang W. Additive manufacturing of metallic components—process, structure and properties. *Prog Mater Sci* 2018;92: 112–224.
- [7] Mittal Sameer, Khan Muztoba Ahmad, Romero David, Wuest Thorsten. A critical review of smart manufacturing & industry 4.0 maturity models: Implications for small and medium-sized enterprises (smes). *J Manuf Syst* 2018;49:194–214.
- [8] Rahman Naveed Ur, Matthews David Thomas Allan, Rooij Matthijn De, Khorasani Amir Mahyar, Gibson Ian, Cordova Laura, Römer Gert-Willem. An overview: laser-based additive manufacturing for high temperature tribology. *Frontiers in Mechanical Engineering* 2019;5(16).
- [9] Tao Fei, Qi Qinglin, Liu Ang, Kusiak Andrew. Data-driven smart manufacturing. *J Manuf Syst* 2018;48:157–69.
- [10] Sharp Michael, Ak Ronay, Jr Thomas Hedberg. A survey of the advancing use and development of machine learning in smart manufacturing. *J Manuf Syst* 2018;48: 170–9.
- [11] Avci Onur, Abdeljaber Osama, Kiranyaz Serkan, Hussein Mohammed, Gabboj Moncef, Inman Daniel J. A review of vibration-based damage detection in civil structures: From traditional methods to machine learning and deep learning applications. *Mech Syst Signal Process* 2021;147:107077.
- [12] Kumar Rakesh, Kumar Manoj, Chohan Jagdeep Singh. The role of additive manufacturing for biomedical applications: a critical review. *J Manuf Process* 2021;64:828–50.
- [13] Wang Jinjiang, Ma Yulin, Zhang Laibin, Gao Robert X, Wu Dazhong. Deep learning for smart manufacturing: methods and applications. *Journal of Manufacturing Systems* 2018;48:144–56.
- [14] Machine learning in additive manufacturing: A reviewMeng Lingbin, McWilliams Brandon, Jarosinski William, Park Hye-Yeong, Jung Yeon-Gil, Lee Jeyyun, Zhang Jing, editors. *JOM* 2020;1–15.
- [15] Jiang Jingchao, Weng Fei, Gao Shiming, Stringer Jonathan, Xun Xu, Guo Ping. A support interface method for easy part removal in directed energy deposition. *Manuf Lett* 2019;20:30–3.
- [16] Bhatia Shaleen. Effect of machine positional errors on geometric tolerances in additive manufacturing. University of Cincinnati; 2014. PhD thesis.
- [17] Zhu HH, Lu L, Fuh JYH. Study on shrinkage behaviour of direct laser sintering metallic powder. *Proc Ins Mech Eng B: J Eng Manuf* 2006;220(2):183–90.
- [18] Ning Y, Wong YS, Fuh Jerry YH, Loh Han Tong. An approach to minimize build errors in direct metal laser sintering. *IEEE Trans Autom Sci Engineering* 2006;3 (1):73–80.
- [19] Paul Ratnadeep. Modeling and optimization of powder based additive manufacturing (AM) processes. PhD thesis. University of Cincinnati; 2013.

- [20] Nasab Milad Hamidi, Gastaldi Dario, Lecis Nora Francesca, Vedani Maurizio. On morphological surface features of the parts printed by selective laser melting (slm). *Addit Manuf* 2018;24:373–7.
- [21] Townsend Andrew, Senin N, Blunt Liam, Leach RK, Taylor JS. Surface texture metrology for metal additive manufacturing: a review. *Precision Engineering* 2016;46:34–47.
- [22] Chan Kwai S, Koike Marie, Mason Robert L, Okabe Toru. Fatigue life of titanium alloys fabricated by additive layer manufacturing techniques for dental implants. *Metall Mater Trans A* 2013;44(2):1010–22.
- [23] Aboulkhair Nesma T, Everitt Nicola M, Ashcroft Ian, Tuck Chris. Reducing porosity in alsi10mg parts processed by selective laser melting. *Addit Manuf* 2014;1:77–86.
- [24] Yuan Lang. Solidification defects in additive manufactured materials. *JOM* 2019; 71(9):3221–2.
- [25] Thijss Lore, Verhaeghe Frederik, Craeghs Tom, Van Humbeeck Jan, Kruth Jean-Pierre. A study of the microstructural evolution during selective laser melting of ti-6al-4v. *Acta Mater* 2010;58(9):3303–12.
- [26] Vilardo Thomas, Colin Christophe, Bartout Jean-Dominique. As-fabricated and heat-treated microstructures of the ti-6al-4v alloy processed by selective laser melting. *Metall Mater Trans A* 2011;42(10):3190–9.
- [27] Gong Haijun, Rafi Khalid, Hengfeng Gu, Starr Thomas, Stucker Brent. Analysis of defect generation in Ti-6Al-4V parts made using powder bed fusion additive manufacturing processes. *Addit Manuf* 2014;1:87–98.
- [28] Mukherjee T, DebRoy T. Mitigation of lack of fusion defects in powder bed fusion additive manufacturing. *J Manuf Process* 2018;36:442–9.
- [29] Liu Qian Chu, Elambasseri Joe, Sun Shou Jin, Leary Martin, Brandt Milan, Sharp Peter Khan. The effect of manufacturing defects on the fatigue behaviour of ti-6al-4v specimens fabricated using selective laser melting. In: *Advanced Materials Research*. 891. Trans Tech Publ; 2014. p. 1519–24.
- [30] Zhou Xin, Wang Dianzheng, Liu Xihe, Zhang DanDan, Shilian Qu, Ma Jing, London Gary, Shen Zhijian, Liu Wei. 3d-imaging of selective laser melting defects in a Co-Cr-Mo alloy by synchrotron radiation micro-ct. *Acta Mater* 2015;98: 1–16.
- [31] Sabau Adrian S, Yuan Lang, Raghavan Narendran, Bement Matthew, Simunovic Srdjan, Turner John A, Gupta Vipul K. Fluid dynamics effects on microstructure prediction in single-laser tracks for additive manufacturing of in625. In: *Metall Mater Trans B*; 2020. p. 1–19.
- [32] Dongdong Gu, Hagedorn Yves-Christian, Meiners Wilhelm, Meng Guangbin, Batista Rui João Santos, Wissenbach Konrad, Poprawe Reinhart. Densification behavior, microstructure evolution, and wear performance of selective laser melting processed commercially pure titanium. *Acta Mater* 2012;60(9):3849–60.
- [33] Zhang Sheng, Gui Rui-zhi, Wei QS, Shi Y. Cracking behavior and formation mechanism of tc4 alloy formed by selective laser melting. *Journal of Mechanical Engineering* 2013;49(23):21–7.
- [34] Mahmoudi Mohamad, Ezzat Ahmed Aziz, Elwany Alaa. Layerwise anomaly detection in laser powder-bed fusion metal additive manufacturing. *Journal of Manufacturing Science and Engineering* 2019;141(3).
- [35] Gaja Haythem, Liou Frank. Defect classification of laser metal deposition using logistic regression and artificial neural networks for pattern recognition. *Int J Adv Manuf Technol* 2018;94(1–4):315–26.
- [36] Tapia G, Elwany AH, Sang H. Prediction of porosity in metal-based additive manufacturing using spatial gaussian process models. *Addit Manuf* 2016;12: 282–90.
- [37] Ye DS, Fuh YHJ, Zhang YJ, Hong GS, Zhu KP. Defects recognition in selective laser melting with acoustic signals by svm based on feature reduction. *MS&E* 2018;436(1):012020.
- [38] Khanzadeh Mojtaba, Chowdhury Sudipta, Marufuzzaman Mohammad, Tschopp Mark A, Bian Linkan. Porosity prediction: Supervised-learning of thermal history for direct laser deposition. *J Manuf Systems* 2018;47:69–82.
- [39] Seifi Seyyed Hadi, Tian Wenmeng, Doude Haley, Tschopp Mark A, Bian Linkan. Layer-wise modeling and anomaly detection for laser-based additive manufacturing. *Journal of Manufacturing Science and Engineering* 2019;141(8).
- [40] Scime Luke, Beuth Jack. Using machine learning to identify in-situ melt pool signatures indicative of flaw formation in a laser powder bed fusion additive manufacturing process. *Addit Manuf* 2019;25:151–65.
- [41] Petrich Jan, Goert Christian, Phoha Shashi, Nassar Abdalla R, Reutzel Edward W. Machine learning for defect detection for pfbam using high resolution layerwise imaging coupled with post-build ct scans. In: *Proceedings of the 27th international solid freeform fabrication symposium*; 2017.
- [42] Imani Farhad, Gaikwad Aniruddha, Montazeri Mohammad, Rao Prahalada, Yang Hui, Reutzel Edward. Process mapping and in-process monitoring of porosity in laser powder bed fusion using layerwise optical imaging. *J Manuf Sci Eng* 2018;140(10).
- [43] Zhang Yingjie, Hong Geok Soon, Ye Dongsen, Zhu Kunpeng, Fuh Jerry YH. Extraction and evaluation of melt pool, plume and spatter information for powder-bed fusion am process monitoring. *Mater Des* 2018;156:458–69.
- [44] Goert Christian, Reutzel Edward W, Petrich Jan, Nassar Abdalla R, Phoha Shashi. Application of supervised machine learning for defect detection during metallic powder bed fusion additive manufacturing using high resolution imaging. *Addit Manuf* 2018;21:517–28.
- [45] Lu ZL, Li DC, Lu BH, Zhang AF, Zhu GX, Pi G. The prediction of the building precision in the laser engineered net shaping process using advanced networks. *Opt Lasers Eng* 2010;48(5):519–25.
- [46] Aminzadeh Masoumeh, Kurfess Thomas R. Online quality inspection using bayesian classification in powder-bed additive manufacturing from high-resolution visual camera images. *J Intell Manuf* 2019;30(6):2505–23.
- [47] Bartlett Jamison L, Jarama Alex, Jones Jonaaron, Li Xiaodong. Prediction of microstructural defects in additive manufacturing from powder bed quality using digital image correlation. *Mater Sci Eng A* 2020;794:140002.
- [48] Montazeri Mohammad, Nassar Abdalla R, Dunbar Alexander J, Rao Prahalada. In-process monitoring of porosity in additive manufacturing using optical emission spectroscopy. *IISETransactions* 2020;52(5):500–15.
- [49] Chen Lequn, Yao Xiling, Xu Peng, Moon Seung Ki, Bi Guijun. Rapid surface defect identification for additive manufacturing with in-situ point cloud processing and machine learning. *Virtual and Physical Prototyping* 2020;1–18.
- [50] García-Moreno Angel-Iván, Alvarado-Orozco Juan-Manuel, Ibarra-Medina Juansethi, Martínez-Franco Enrique. Image-based porosity classification in al-alloys by laser metal deposition using random forests. *Int J Adv Manuf Technol* 2020;110(9):2827–45.
- [51] Öznel Tuğrul, Altay Ayça, Kaftanoğlu Bilgin, Leach Richard, Senin Nicola, Donmez Alkan. Focus variation measurement and prediction of surface texture parameters using machine learning in laser powder bed fusion. *J Manuf Sci Eng* 2020;142(1).
- [52] Gaikwad Aniruddha, Giera Brian, Guss Gabriel M, Forien Jean-Baptiste, Matthews Manyalibjo J, Rao Prahalada. Heterogeneous sensing and scientific machine learning for quality assurance in laser powder bed fusion—a single-track study. *Addit Manuf* 2020;36:101659.
- [53] Imani Farhad, Chen Ruimin, Diewald Evan, Reutzel Edward, Yang Hui. Deep learning of variant geometry in layerwise imaging profiles for additive manufacturing quality control. *J Manuf Sci Eng* 2019;141(11).
- [54] Yazdi Reza Mojahed, Imani Farhad, Yang Hui. A hybrid deep learning model of process-build interactions in additive manufacturing. *J Manuf Syst* 2020;57: 460–8.
- [55] Cui Wenyuan, Zhang Yunlu, Zhang Xinchang, Li Lan, Liou Frank. Metal additive manufacturing parts inspection using convolutional neural network. *Appl Sci* 2020;10(2):545.
- [56] Gaikwad Aniruddha, Imani Farhad, Yang Hui, Reutzel Edward, Rao Prahalada. In situ monitoring of thin-wall build quality in laser powder bed fusion using deep learning. 2019.
- [57] Kunkel Maximilian Hugo, Gebhardt Andreas, Mpofu Khumbulani, Kallweit Stephan. Quality assurance in metal powder bed fusion via deep-learning-based image classification. *Rapid Prototyp J* 2019;26(2):259–66.
- [58] Yuan Bodu, Guss Gabriel M, Wilson Aaron C, Hau-Riege Stefan P, DePond Phillip J, McMains Sara, Matthews Manyalibjo J, Giera Brian. Machine-learning-based monitoring of laser powder bed fusion. *Advanced Materials Technologies* 2018;3 (12):1800136.
- [59] Zhang Binbin, Jaiswal Prakhar, Rai Rahul, Guerrier Paul, Baggs George. Convolutional neural network-based inspection of metal additive manufacturing parts. *Rapid Prototyping Journal* 2019;25(3):530–40.
- [60] Gonzalez-Val Carlos, Pallas Adrian, Panadeiro Veronica, Rodriguez Alvaro. A convolutional approach to quality monitoring for laser manufacturing. *J Intell Manuf* 2020;31(3):789–95.
- [61] Zhang Bin, Liu Shunyu, Shin Yung C. In-process monitoring of porosity during laser additive manufacturing process. *Addit Manuf* 2019;28:497–505.
- [62] Tian Qi, Gue Shenghan, Guo Yuebin, et al. A physics-driven deep learning model for process-porosity causal relationship and porosity prediction with interpretability in laser metal deposition. *CIRP Annals* 2020;69(1):205–8.
- [63] Li Xiang, Siahpour Shahin, Lee Jay, Wang Yachao, Shi Jing. Deep learning-based intelligent process monitoring of directed energy deposition in additive manufacturing with thermal images. *Procedia Manuf* 2020;48:643–9.
- [64] Scime Luke, Siddle Derek, Baird Seth, Paquit Vincent. Layer-wise anomaly detection and classification for powder bed additive manufacturing processes: A machine-agnostic algorithm for real-time pixel-wise semantic segmentation. *Additive Manufacturing* 2020;101453. PhD thesis.
- [65] Xiao Ling, Mingyan Lu, Huang Han. Detection of powder bed defects in selective laser sintering using convolutional neural network. *Int J Adv Manuf Technol* 2020;1–12.
- [66] Scime Luke, Beuth Jack. A multi-scale convolutional neural network for autonomous anomaly detection and classification in a laser powder bed fusion additive manufacturing process. *Addit Manuf* 2018;24:273–86.
- [67] Zhang Yingjie, Soon Hong Geok, Ye Dongsen, Fuh Jerry Ying Hsi, Zhu Kunpeng. Powder-bed fusion process monitoring by machine vision with hybrid convolutional neural networks. *IEEE Transactions on Industrial Informatics* 2019; 16(9):5769–79.
- [68] Francis Jack, Bian Linkan. Deep learning for distortion prediction in laser-based additive manufacturing using big data. *Manuf Lett* 2019;20:10–4.
- [69] Caggiano Alessandra, Zhang Jianjing, Alfieri Vittorio, Caiazzo Fabrizia, Gao Robert, Teti Roberto. Machine learning-based image processing for on-line defect recognition in additive manufacturing. *CIRP Ann* 2019;68(1):451–4.
- [70] Han Feng, Zou Jingling, Ai Yuan, Xu Chunlin, Liu Sheng. Image classification and analysis during the additive manufacturing process based on deep convolutional neural networks. In: *2019 20th International Conference on Electronic Packaging Technology (ICEPT)*. IEEE; 2019. p. 1–4.
- [71] Williams Jacob, Dryburgh Paul, Clare Adam, Rao Prahalada, Samal Ashok. Defect detection and monitoring in metal additive manufactured parts through deep learning of spatially resolved acoustic spectroscopy signals. 2018.
- [72] Li Yuemeng, Yan Hairong, Zhang Yuefei. A deep learning method for material performance recognition in laser additive manufacturing. In: *2019 IEEE 17th international conference on industrial informatics (INDIN)*. 1. IEEE; 2019. p. 1735–40.

- [73] Baumgartl Hermann, Tomas Josef, Buettner Ricardo, Merkel Markus. A deep learning-based model for defect detection in laser-powder bed fusion using in-situ thermographic monitoring. *Progress in Additive Manufacturing* 2020;1–9.
- [74] Shevchik Sergey A, Kenel Christoph, Leinenbach Christian, Wasmer Kilian. Acoustic emission for in situ quality monitoring in additive manufacturing using spectral convolutional neural networks. *Addit Manuf* 2018;21:598–604.
- [75] Tian Qi, Guo Shenghan, Melder Erika, Bian Linkan, Guo Weihong, et al. Deep learning-based data fusion method for in situ porosity detection in laser-based additive manufacturing. *J Manuf Sci Eng* 2021;143(4).
- [76] Hertlein Nathan, Deshpande Sourabh, Venugopal Vysakh, Kumar Manish, Anand Sam. Prediction of selective laser melting part quality using hybrid bayesian network. *Addit Manuf* 2020;32:101089.
- [77] Kwon Ohhyung, Kim Hyung Giun, Ham Min Ji, Kim Wonrae, Kim Gun-Hee, Cho Jae-Hyung, Kim Nam Il, Kim Kangil. A deep neural network for classification of melt-pool images in metal additive manufacturing. *J Intelligent Manuf* 2020;31(2):375–86.
- [78] Mohammadi Mohammad Ghayoomi, Mahmoud Dalia, Elbestawi Mohamed. On the application of machine learning for defect detection in l-pbf additive manufacturing. *Opt Laser Technol* 2021;143:107338.
- [79] Mahamood Rasheedat M, Akinlabi Esther T, Owolabi Moses G. Effect of laser power and powder flow rate on dilution rate and surface finish produced during laser metal deposition of titanium alloy. In: 2017 8th international conference on mechanical and intelligent manufacturing technologies (ICMIMT). IEEE; 2017. p. 6–10.
- [80] He Kaiming, Zhang Xiangyu, Ren Shaobo, Sun Jian. Deep residual learning for image recognition. In: Proceedings of the IEEE conference on computer vision and pattern recognition; 2016. p. 770–8.
- [81] Shevchik Sergey A, Masinelli Giulio, Kenel Christoph, Leinenbach Christian, Wasmer Kilian. Deep learning for in situ and real-time quality monitoring in additive manufacturing using acoustic emission. *IEEE Trans Ind Inform* 2019;15(9):5194–203.
- [82] Scime Luke, Beuth Jack. Anomaly detection and classification in a laser powder bed additive manufacturing process using a trained computer vision algorithm. *Addit Manuf* 2018;19:114–26.
- [83] Snell Robert, Tammas-Williams Sam, Chechik Lova, Lyle Alistair, Hernández-Nava Everth, Boig Charlotte, Panoutsos George, Todd Iain. Methods for rapid pore classification in metal additive manufacturing. *JOM* 2020;72(1):101–9.
- [84] Grasso Marco, Laguzza Vittorio, Semeraro Quirico, Colosimo Bianca Maria. In-process monitoring of selective laser melting: spatial detection of defects via image data analysis. *Journal of Manufacturing Science and Engineering* 2017;139(5).
- [85] Yadav Pinku, Singh Vibhutesh Kumar, Joffre Thomas, Rigo Olivier, Arvie Corinne, Guen Emilie Le, Lacoste Eric. Inline drift detection using monitoring systems and machine learning in selective laser melting. *Advanced Engineering Materials* 2020;2000660.
- [86] Gaja Haythem, Liou Frank. Defects monitoring of laser metal deposition using acoustic emission sensor. *Int J Adv Manuf Technol* 2017;90(1–4):561–74.
- [87] Taheri Hossein, Koester Lucas W, Bigelow Timothy A, Faierson Eric J, Bond Leonard J. In situ additive manufacturing process monitoring with an acoustic technique: clustering performance evaluation using k-means algorithm. *J Manuf Sci Eng* 2019;141(4).
- [88] Ren Wenjing, Wen Guangrui, Zhang Zhifan, Mazumder Jyoti. Quality monitoring in additive manufacturing using emission spectroscopy and unsupervised deep learning. *Mater Manuf Process* 2021;1–8.
- [89] Ye Dongsen, Hong Geok Soon, Zhang Yingjie, Zhu Kunpeng, Fuh Jerry Ying Hsi. Defect detection in selective laser melting technology by acoustic signals with deep belief networks. *The International Journal of Advanced Manufacturing Technology* 2018;96(5–8):2791–801.
- [90] Ye Dongsen, Fuh Jerry Ying Hsi, Zhang Yingjie, Hong Geok Soon, Zhu Kunpeng. In situ monitoring of selective laser melting using plume and sputter signatures by deep belief networks. *ISA Transactions* 2018;81:96–104.
- [91] García-Moreno Angel-Iván. Automatic quantification of porosity using an intelligent classifier. *Int J Adv Manuf Technol* 2019;105(5):1883–99.
- [92] Khanzadeh Mojtaba, Chowdhury Sudipta, Tschoop Mark A, Doude Haley R, Marufuzzaman Mohammad, Bian Linkan. In-situ monitoring of melt pool images for porosity prediction in directed energy deposition processes. *IIE Transactions* 2019;51(5):437–55.
- [93] Okaro Ikenna A, Jayasinghe Sarini, Sutcliffe Chris, Black Kate, Paoletti Paolo, Green Peter L. Automatic fault detection for laser powder-bed fusion using semi-supervised machine learning. *Addit Manuf* 2019;27:42–53.
- [94] Yuan Bodhi, Giera Brian, Guse Gabe, Matthews Ibo, McMains Sara. Semi-supervised convolutional neural networks for in-situ video monitoring of selective laser melting. In: 2019 IEEE winter conference on applications of computer vision (WACV). IEEE; 2019. p. 744–53.
- [95] Li Xiang, Jia Xiaodong, Yang Qibo, Lee Jay. Quality analysis in metal additive manufacturing with deep learning. *J Intell Manuf* 2020;1–15.
- [96] Wasmer K, Le-Quang T, Meylan B, Shevchik SA. In situ quality monitoring in am using acoustic emission: a reinforcement learning approach. *J MaterEng Perform* 2019;28(2):666–72.
- [97] Yao Bing, Yang Hui. Constrained markov decision process modeling for sequential optimization of additive manufacturing build quality. *IEEE Access* 2018;6:54786–94.
- [98] Wang Chengcheng, Tan XP, Tor SB, Lim CS. Machine learning in additive manufacturing: state-of-the-art and perspectives. *Additive Manufacturing* 2020; 101538.
- [99] Razvi Sayeda Saadia, Feng Shaw, Narayanan Anantha, Lee Yung-Tsun Tina, Witherell Paul. A review of machine learning applications in additive manufacturing. In: International Design Engineering Technical Conferences and Computers and Information in Engineering Conference. 59179. American Society of Mechanical Engineers; 2019. page V001T02A040.
- [100] Karniadakis George Em, Kevrekidis Ioannis G, Lu Lu, Perdikaris Paris, Wang Sifan, Yang Liu. Physics-informed machine learning. *Nature Reviews Physics* 2021;3(6):422–40.
- [101] Faruque Mohammad Abdullah Al, Chhetri Sujit Rokka, Canedo Arquimedes, Wan Jiang. Acoustic side-channel attacks on additive manufacturing systems. In: 2016 ACM/IEEE 7th international conference on cyber-physical systems (ICCPs). IEEE; 2016. p. 1–10.
- [102] Molitch-Hou Michael. Overview of additive manufacturing process. In: *Additive Manufacturing*. Elsevier; 2018. p. 1–38.
- [103] Schmidt Michael, Merklein Marion, Bourell David, Dimitrov Dimitri, Hausotte Tina, Wegener Konrad, Overmeyer Ludger, Vollertsen Frank, Levy Gideon N. Laser based additive manufacturing in industry and academia. *Cirp Annals* 2017;66(2):561–83.
- [104] Yosinski Jason, Clune Jeff, Bengio Yoshua, Lipson Hod. How transferable are features in deep neural networks?. In: arXiv preprint; 2014. arXiv:1411.1792.